

Intersubband polaritons in the electrical dipole gauge

Yanko Todorov and Carlo Sirtori

Laboratoire "Matériaux et Phénomènes Quantiques", Université Paris Diderot-Paris 7, CNRS-UMR 7162, FR-75013 Paris, France

(Received 5 September 2011; revised manuscript received 22 November 2011; published 6 January 2012)

We provide a theoretical description of the coupling between the electromagnetic field and the intersubband excitations of a bidimensional electron gas. Our theory, based on the electrical dipole gauge, applies generally to an arbitrary quantum heterostructure embedded in a multilayer waveguide or in a microcavity. We show that the dipole gauge Hamiltonian takes into account the Coulomb interactions in the system, without the need of adding extra terms to the Hamiltonian. Furthermore, the bright excitations of the system appear as many-body collective plasmon modes, interacting between each other and with the light field through dipole coupling. The electrical dipole gauge therefore provides a suitable framework for the study of solid-state quantum electrodynamics phenomena that occur at very high electronic densities, such as the ultrastrong light-matter interaction.

DOI: [10.1103/PhysRevB.85.045304](https://doi.org/10.1103/PhysRevB.85.045304)

PACS number(s): 71.36.+c, 73.21.-b, 78.20.Bh

I. INTRODUCTION

In the description of a physical problem dealing with light-matter interaction, there is always a degree of freedom in the choice of the potentials associated with the electromagnetic field. Even though the physical phenomena are obviously independent from the particular vector or scalar potentials used, the choice of the gauge is a critical issue, as it can be more or less adequate for the physical interpretation of the phenomena. In the literature, there is already a consensus that the interaction of nonrelativistic bound charges is very conveniently expressed in terms of the dipole gauge.¹ This has been first identified by Power and Zienau in the 1950s (Ref. 2) and subsequently by Woolley.³ In this formulation, called Power-Zienau-Woolley (PZW) gauge, the sources are electric and magnetic polarization fields and the coupling occurs via the intensities of the displacement field \mathbf{D} and the magnetic field \mathbf{H} rather than using the scalar and vector potentials V and \mathbf{A} . In the case where the magnetic interactions in the system can be neglected, the PZW gauge is also called dipole gauge since the interaction Hamiltonian contains only the coupling between the material polarization \mathbf{P} with the light field.

In our paper, we propose to apply the dipole gauge to the case of intersubband transitions interacting with a photonic cavity mode. The motivation of our approach stems from the fact that we are interested to investigate a regime, called ultrastrong coupling, first introduced by Ciuti *et al.*⁴ This regime of light-matter interaction is attainable in a bidimensional electron gas with very high density embedded into a photonic microcavity⁴⁻⁶ and is characterized by the fact that the coupling and the material excitation energies are comparable quantities. However, the very high electronic densities increase on one hand the light-matter interaction and on the other renormalize the transition energies of the system due to a collective effect, the "depolarization shift."⁷ This effect can not be neglected in the limit of ultrastrong coupling, however, it was not explicitly considered in the initial study described in Ref. 4. In our work, we show that the dipole gauge Hamiltonian handles the light-matter interaction and the depolarization effect on the same footing. The underlying physical picture is that the active polarization that couples to the photonic mode is not a single-particle electronic transition between confined states, but rather a collective electronic

mode (a plasmonic mode) arising from electrons distributed in different subbands, yet phased by the Coulomb interaction. The latter point is one of the main conclusions of our theoretical investigation.

The correct description of the collective electronic excitations and their interaction with light can be obtained in the Coulomb gauge, only if both the vector potential \mathbf{A} and scalar potential V are considered. This has already been noticed in studies of ensembles of two-level systems interacting with light.⁸ In the absence of the cavity, thus in the weak-coupling limit, collective effects can be identified with the scalar potential V ,⁹ which describes an instantaneous interaction between electrons.¹⁰ However, when dealing with the resonant coupling of a microcavity with an electronic transition the observable quantity is the retarded electromagnetic field that can be obtained through a proper combination of both V and \mathbf{A} .¹⁰ In order to have a general Hamiltonian, which is valid from the weak- to the ultrastrong-coupling regimes, it is therefore essential to include the Coulomb potential V , thus completing the study of Ref. 4. Such Hamiltonian is readily obtained in the dipole gauge, where the matter degrees of freedom are gathered in the polarization field \mathbf{P} , which not only describes the interactions between the electrons, but also couples to a material-independent and retarded photonic field described by the electric displacement \mathbf{D} .^{1,10} Indeed, as we previously pointed out in Ref. 6, the depolarization effect in the bidimensional electron gas is contained in the quadratic \mathbf{P}^2 term of the dipolar Hamiltonian. As a result, our model correctly describes the local field effects arising from the very different spatial scales between the electronic and photonic confinements. The results of Ref. 4 are contained in our formalism and recovered only in the opposite limit, i.e., when the electronic polarization fills the whole cavity volume. The importance of the spatial overlap factor was also outlined in our experimental study of the ultrastrong-coupling regime^{6,11} as it allows us to correlate both polaritonic and weak-coupling absorption data. On a more fundamental level, we show how the spatial confinement of the electronic polarization leads to the no-go theorem for intersubband transitions.^{12,13}

Our paper is organized as follows. In Sec. II, we establish the Hamiltonian of the system in the dipole gauge. We consider a very general case of an arbitrary heterostructure

embedded into a general planar waveguide multilayer. The microscopic expression of the intersubband polarization field is derived in Sec. II D, in the long-wavelength approximation. This microscopic expression relies directly on the electronic wave functions, and therefore allows us to go beyond the semiclassical model employed in Ref. 6, as it applies to an arbitrary heterostructure potential, with an arbitrary number of occupied subbands.

In Sec. III, we adapt the general dipolar Hamiltonian obtained in Sec. II to the case of a series of highly doped quantum wells and we express it in terms of the collective electronic excitations of the system. We also provide a version of this “plasma Hamiltonian” for the case of zero-dimensional (0D) resonators (Sec. III C). In Sec. III D, we study the correspondence between the plasma Hamiltonian, truncated for the case of a single intersubband transition and a single waveguide mode, and the corresponding Hamiltonian in the Coulomb gauge. This allows us to connect our formalism with previous work.⁴ In particular, we show that the dipole gauge provides automatically the relevant contributions due to the Coulomb interaction of the system, which were missing in Ref. 4.

The formalism is applied to study the properties of the polariton states in Sec. IV. In Sec. IV A, we examine the polariton dispersion, and in Sec. IV B, we discuss the no-go theorem for intersubband transitions. We show in Sec. IV C that our formalism is consistent with the effective medium approach, in full agreement with what has been proposed in the literature.¹⁴ Most of the technical details have been gathered in the appendices.

II. INTERACTION HAMILTONIAN

A. General considerations

The interaction between light and quantum heterostructures is usually studied in planar multilayered systems. This geometry is most naturally compatible with the epitaxial growth. A very general system is described in Fig. 1(a). It consists of homogeneous, nonabsorbing, and nondispersive dielectric layers described by real dielectric constants ε_i , embedded between two infinite semiplanes that act as optical claddings. We can then define a piecewise dielectric function $\varepsilon(z)$, with $\varepsilon(z) = \varepsilon_i$ in the i th layer, z being the growth axis. The multilayered dielectric stack defines guided modes that confine the light field around the heterostructures. Note that, at this point, $\varepsilon(z)$ does not include the resonant contribution from the electronic transition in the heterostructures. This contribution will be included through the coupling between the guided modes and the electronic polarization. The full Hamiltonian of the system is written as

$$\hat{H} = \hat{H}_e + \hat{H}_p + \hat{H}_{\text{int}}. \quad (1)$$

Here, \hat{H}_e is the Hamiltonian of the electron gas in the heterostructures, which is provided explicitly in Sec. II C, and \hat{H}_p is the photon Hamiltonian:

$$\hat{H}_p = \int \left[\frac{1}{2\varepsilon_0\varepsilon(z)} \hat{\mathbf{D}}^2(\mathbf{r}) + \frac{\mu_0}{2} \hat{\mathbf{H}}^2(\mathbf{r}) \right] d^3\mathbf{r} \quad (2)$$

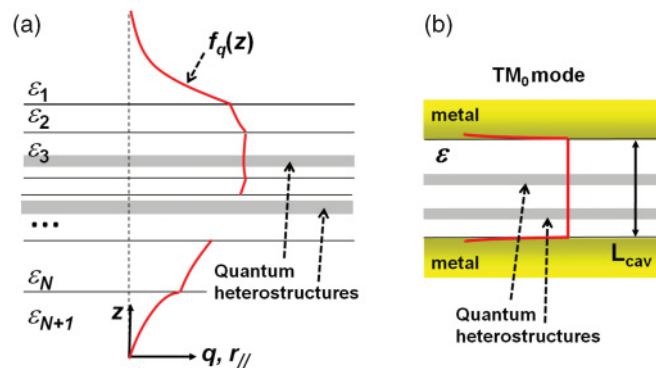


FIG. 1. (Color online) (a) General planar multilayered system with a piecewise dielectric function $\varepsilon(z)$, supporting guided modes. There are quantum heterostructures embedded inside the multilayered stack. (b) TM_0 mode guided between two metallic plates.

with $\hat{\mathbf{D}}(\mathbf{r})$ and $\hat{\mathbf{H}}(\mathbf{r})$, respectively, the displacement field and the magnetic field operators. The interaction Hamiltonian \hat{H}_{int} in the electrical dipole gauge is written as, neglecting the magnetic interactions,¹⁵

$$\hat{H}_{\text{int}} = \int \frac{1}{\varepsilon_0\varepsilon(z)} \left[-\hat{\mathbf{D}}(\mathbf{r}) \cdot \hat{\mathbf{P}}(\mathbf{r}) + \frac{1}{2} \hat{\mathbf{P}}^2(\mathbf{r}) \right] d^3\mathbf{r}. \quad (3)$$

Here, $\hat{\mathbf{P}}(\mathbf{r})$ is the polarization density operator of the electron gas. This is a central quantity in our theory, and it is provided explicitly in Sec. II D from a microscopic model. One issue that we will discuss in details in the paper is the role of the quadratic interaction term $\hat{\mathbf{P}}^2(\mathbf{r})$, which describes the self-interaction of the electronic polarization, and therefore contains the effects of the dipole-dipole interactions.

Most generally, the expression of the interaction (3) should be written as a nonlocal expression, which takes into account the spatial dispersion of the electromagnetic response of the medium.¹⁶ However, as illustrated in Fig. 1(a), in the systems that we study, the heterostructures embedded in the multilayered stack have a typical extension in the growth axis (the z axis) that is much smaller than the wavelength. This justifies the local form of the interaction postulated in Eq. (3).

We can evaluate the convenience of the dipole gauge already at the classical level, where the displacement field $\mathbf{D}(\mathbf{r})$ is determined only by the charges exterior to the system. On a quantum mechanical level, this means that $\hat{\mathbf{D}}(\mathbf{r})$ describes a purely transverse field.¹⁰ Therefore, neglecting the dissipation in the system, we can consider $\hat{\mathbf{D}}(\mathbf{r})$ as a free photon field, independent from the electronic polarization of the heterostructures. This can be clearly observed, for instance, in the normal component of the displacement field $\hat{\mathbf{D}}_z$, which, while it couples to the intersubband polarization, is continuous across the interfaces. We therefore consider the derivation of $\hat{\mathbf{D}}(\mathbf{r})$ as a separate problem, which is dependent only on the particular arrangement of the multilayered stack. In this approach, the resonant contributions of the electronic intersubband transitions taking place in the active media are contained separately in the polarization operator density $\hat{\mathbf{P}}$, and are active only through the interaction term \hat{H}_{int} . Later on (Sec. IV C), we shall see that this approach leads to an effective medium treatment of the system.

In our treatment, the dissipation effects will be neglected. The latter can be taken into account as in the classical paper by Huttner and Barnett¹⁷ by including a dissipative bath with continuous degrees of freedom. This approach will, however, require more precise definition of the displacement field $\hat{\mathbf{D}}$, as it leads to a noise contribution from the dissipative bath.^{15,17} Here, we will restrict to a fully Hamiltonian treatment. The dissipation will be taken into account only in a phenomenological way in Sec. IV C by adding a small imaginary part to the eigenfrequencies of the system.¹⁸

B. Free photon Hamiltonian

For the quantum description of electromagnetic field, we use the basis of the guided modes of the multilayered stack, which are bounded in space. Due to the translational invariance of the system in the plane perpendicular to the z axis, the guided modes are characterized by their in-plane wave vector \mathbf{q} and their energy $\hbar\omega_{c\mathbf{q}}$. The function $\omega_{c\mathbf{q}} = \omega_{c\mathbf{q}}(|\mathbf{q}|)$ defines the dispersion relation of the guided modes. The heterostructures interact only with the Transverse Magnetic (TM)-polarized modes in order to respect the selection rule of intersubband transitions.¹⁹ By using the general quantization rules,^{10,20} we can assign bosonic creation and annihilation operators $a_{\mathbf{q}}^\dagger$ and $a_{\mathbf{q}}$ to each guided mode. The components of the quantized electromagnetic TM free field are then

$$\hat{\mathbf{H}} = \sum_{\mathbf{q}} i A_{\mathbf{q}} (\mathbf{e}_{\mathbf{q}} \wedge \mathbf{e}_z) f_{\mathbf{q}}(z) e^{i\mathbf{q}\mathbf{r}_{\parallel}} (a_{\mathbf{q}} + a_{-\mathbf{q}}^\dagger), \quad (4)$$

$$\hat{\mathbf{D}}_z = \sum_{\mathbf{q}} i A_{\mathbf{q}} \mathbf{e}_z \frac{|\mathbf{q}|}{\omega_{c\mathbf{q}}} f_{\mathbf{q}}(z) e^{i\mathbf{q}\mathbf{r}_{\parallel}} (a_{\mathbf{q}} - a_{-\mathbf{q}}^\dagger), \quad (5)$$

$$\hat{\mathbf{D}}_{\parallel} = - \sum_{\mathbf{q}} A_{\mathbf{q}} \mathbf{e}_{\mathbf{q}} \frac{1}{\omega_{c\mathbf{q}}} \frac{df_{\mathbf{q}}(z)}{dz} e^{i\mathbf{q}\mathbf{r}_{\parallel}} (a_{\mathbf{q}} - a_{-\mathbf{q}}^\dagger), \quad (6)$$

$$A_{\mathbf{q}} = \left(\frac{\hbar\omega_{c\mathbf{q}}}{2\mu_0 S L_{\mathbf{q}}} \right)^{1/2}. \quad (7)$$

Here, S is the area of the system and \mathbf{r}_{\parallel} is the in-plane position vector. We have introduced the unit vectors \mathbf{e}_z and $\mathbf{e}_{\mathbf{q}} = \mathbf{q}/|\mathbf{q}|$, and the symbol \wedge designs the vector product. The constant $A_{\mathbf{q}}$ is the vacuum field intensity of the guided modes. It has been derived, for this particular system, in Appendix A. The function $f_{\mathbf{q}}(z)$ describes the lateral profile of the guided modes, and $L_{\mathbf{q}}$ is a normalization coefficient:

$$\int_{-\infty}^{+\infty} f_{\mathbf{q}}(z)^2 dz = L_{\mathbf{q}}. \quad (8)$$

If we set the maximum of the dimensionless function $f_{\mathbf{q}}(z)$ equal to 1, with this definition, $L_{\mathbf{q}}$ can be regarded as the effective thickness of the multilayer system. The function $f_{\mathbf{q}}(z)$ satisfies the Helmholtz equation

$$\frac{d^2 f_{\mathbf{q}}(z)}{dz^2} - \mathbf{q}^2 f_{\mathbf{q}}(z) + \frac{\varepsilon(z)\omega_{c\mathbf{q}}^2}{c^2} f_{\mathbf{q}}(z) = 0. \quad (9)$$

According to the boundary conditions for the electromagnetic field, $f_{\mathbf{q}}$ and $\varepsilon(z)^{-1} df_{\mathbf{q}}/dz$ must be continuous at the interfaces between the different layers, and $f_{\mathbf{q}}(z)$ must vanish for $z \rightarrow \pm\infty$. Such a function has been illustrated in Fig. 1(a). Equation (9) will have in general multiple solutions, describing

different modes labeled by a discrete index j , which can be added in the notations if necessary.

One or two boundaries of the multilayer system can be metallic. In the mid- and far-infrared frequency ranges, the metals are described by a very large negative real dielectric constant $\varepsilon_M < 0$, and the electromagnetic field density in the metallic layers is vanishing. Therefore, in order to have a consistent quantification scheme for the electromagnetic field, without the burden of quantifying the conducting electrons in the metallic boundaries, we neglect the electromagnetic density energy in the metallic regions in the integrals (2) and (3). However, the finite dielectric constant ε_M can be taken into account through the dispersion relation of the guided modes as for the example provided in Appendix A.

With the use of the above expressions, the Hamiltonian (2) of the free electromagnetic field takes the standard form

$$\hat{H}_p = \sum_{\mathbf{q}} \hbar\omega_{c\mathbf{q}} (a_{\mathbf{q}}^\dagger a_{\mathbf{q}} + 1/2). \quad (10)$$

We now apply this formalism to a particular system. For mid-IR and THz frequencies, the simplest confining system is provided by the TM_0 mode guided between two metallic plates, separated by a distance L_{cav} , as illustrated in Fig. 1(b). The semiconductor with a dielectric constant ε fills the space between the plates. In this case, in the limit of perfect metallic boundaries we have $f_{\mathbf{q}}(z) = 1$ and $L_{\mathbf{q}} = L_{\text{cav}}$ and the dispersion relation becomes $\mathbf{q}^2 = \varepsilon\omega_{c\mathbf{q}}^2/c^2$ [Fig. 1(b)]. The in-plane component of the displacement field vanishes, $\hat{\mathbf{D}}_{\parallel} = \mathbf{0}$, and the remaining nonzero z component is

$$\hat{\mathbf{D}}_z = i\mathbf{e}_z \sum_{\mathbf{q}} \sqrt{\frac{\varepsilon\varepsilon_0\hbar\omega_{c\mathbf{q}}}{2SL_{\text{cav}}}} e^{i\mathbf{q}\mathbf{r}_{\parallel}} (a_{\mathbf{q}} - a_{-\mathbf{q}}^\dagger). \quad (11)$$

In the rest of the paper, we consider exclusively the TM_0 mode, which simplifies greatly the calculations without a loss of generality. In Sec. III C, we also consider the case of double-metal zero-dimensional microcavities in which we have added a lateral confinement. In these structures, the propagation wave vector \mathbf{q} of the TM_0 mode becomes quantized.

C. Electronic Hamiltonian

In a semiconductor heterostructure, the band offsets between different semiconductor layers provide a confining potential $V(z)$ in the growth axis. A typical example of a confining heterostructure, the quantum well, is sketched in Fig. 2(a), and a general heterostructure is illustrated in Fig. 2(b). We consider the case where the Fermi level E_F lies into the conduction band, due to intentional doping, which leads to the formation of a bidimensional electron gas⁷ [Fig. 2(b)]. The potential $V(z)$ yields discrete energy levels $\hbar\omega_{\lambda}$, labeled by an integer index λ . Electrons are free to move in the plane perpendicular to the growth axis, and we denote by $\hbar\mathbf{k}$ their in-plane momentum. This free movement is described by the parabolic subbands illustrated in Figs. 2(a) and 2(b), and the total energy of an electron in the subband λ is

$$\hbar\omega_{\lambda\mathbf{k}} = \hbar\omega_{\lambda} + \frac{\hbar^2\mathbf{k}^2}{2m^*} \quad (12)$$

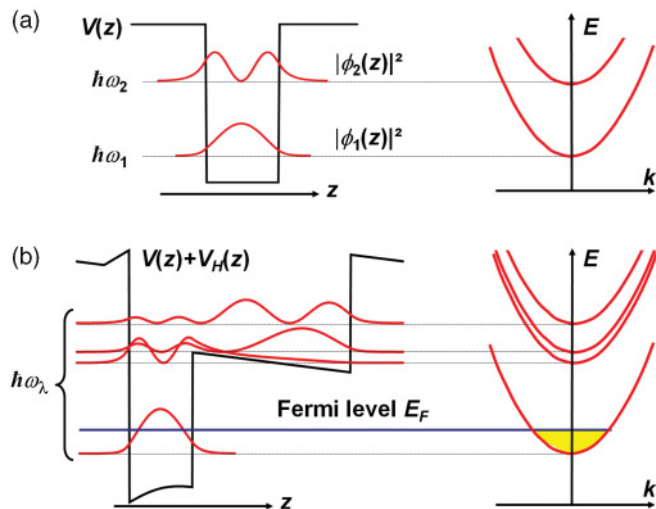


FIG. 2. (Color online) (a) Typical quantum heterostructure potential $V(z)$: a quantum well. There are two bound levels with wave functions $\phi_{1,2}(z)$. (b) General potential of a doped heterostructure, including the Hartree correction $V_H(z)$ due to the static Coulomb interactions.

with m^* the effective electron mass. In a highly doped heterostructure, in order to determine the confining energies $\hbar\omega_\lambda$, one must take into account not only the heterostructure potential, but also the Coulomb interaction between the charges. In the Hartree approximation, this static Coulomb interaction is described by a self-consistent potential $V_H(z)$ due to the presence of electrons and ionized impurities.^{7,19} The potential $V_H(z)$ depends on the envelope wave functions $\phi_\lambda(z)$. Therefore, the energies $\hbar\omega_\lambda$ and wave function $\phi_\lambda(z)$ are determined altogether by solving the one-particle Schrödinger equation with a total potential $V(z) + V_H(z)$ self-consistently with a Poisson problem:⁷

$$\left[-\frac{\hbar^2}{2m^*} \frac{d^2}{dz^2} + V(z) + V_H(z) \right] \phi_\lambda(z) = \hbar\omega_\lambda \phi_\lambda(z), \quad (13)$$

$$\frac{d^2 V_H(z)}{dz^2} = -\frac{e^2}{\epsilon\epsilon_0} [\rho(z) - N_d(z)], \quad (14)$$

$$\rho(z) = \frac{m^*}{\pi\hbar^2} \sum_\lambda N_\lambda |\phi_\lambda(z)|^2. \quad (15)$$

Here, $\rho(z)$ is the electronic density, $N_d(z)$ is the dopant density, and N_λ is the population of the λ th subband. The exchange-correlation effect has been neglected in the above equations. This set of equations leads to one-particle quantum states $|\lambda, \mathbf{k}\rangle$ with normalized wave functions

$$\langle \mathbf{r} | \lambda, \mathbf{k} \rangle = \phi_\lambda(z) \frac{1}{\sqrt{S}} \exp(i\mathbf{k}\mathbf{r}_\parallel). \quad (16)$$

The corresponding fermionic destruction and creation operators are $c_{\lambda\mathbf{k}}$ and $c_{\lambda\mathbf{k}}^\dagger$. The electronic Hamiltonian acquires the one-particle form

$$\hat{H}_e = \sum_{\lambda\mathbf{k}} \hbar\omega_{\lambda\mathbf{k}} c_{\lambda\mathbf{k}}^\dagger c_{\lambda\mathbf{k}}. \quad (17)$$

At this point, we have determined the stationary state of the system. The effects of the Coulomb interaction that we

have considered so far are the static effects arising from the inhomogeneous spatial distribution of charges. These static effects have been lumped into the one-particle subband energies $\hbar\omega_{\lambda\mathbf{k}}$ through the self-consistent set of equations (13)–(15).

In the next section, we use the stationary basis of single-particle states $\phi_\lambda(z)$ in order to define the microscopic polarization density of the electron gas. This will allow us to study the excited collective states, coupled with light, and to recover the dynamic effects of the Coulomb interaction, such as the depolarization shift.

D. Microscopic expression of the polarization

Usually, for the studies of the interaction of intersubband transitions with light, one does not define a polarization operator as an independent local quantity $\hat{\mathbf{P}}(\mathbf{r})$, but rather computes the linear response of the electronic system due to the sollicitation of an external harmonic electric field. The linear response is described by the frequency-dependent nonlocal susceptibility $\chi(\omega)$,²¹ which is computed from the current-current correlation function through the Kubo formula.²² The collective excitations of the system are then obtained from the analytical properties of $\chi(\omega)$.

In order to use the electrical dipole gauge, as formulated by the interaction Hamiltonian (3), we need to express the local polarization operator $\hat{\mathbf{P}}(\mathbf{r})$ as an independent quantity. Classically, the local polarization $\mathbf{P}(\mathbf{r})$ is defined as the average dipole moment of the charge distribution over some microscopic volume.²³ For instance, in the case of the square quantum well with a thickness L_{QW} illustrated in Fig. 2(a), such volume could be the volume of the quantum well. However, it is difficult to apply such a definition for an arbitrary heterostructure, such as the one depicted in Fig. 2(b), where the spatial extension of the confinement potential varies with the energy. In this case, the averaging volume becomes an arbitrary quantity. Since the microscopic intersubband dipole is defined from the electronic wave functions $\phi_\lambda(z)$, the truly microscopic expression of $\hat{\mathbf{P}}(\mathbf{r})$ should involve directly $\phi_\lambda(z)$.

A similar problem has been encountered in the attempts to define the static polarization in ferromagnetic materials as function of the electronic wave functions and nuclei distributions.²⁴ Then, the idea is to define the polarization as the time integral of the microscopic current arising during the adiabatic switch from one configuration of electrons and nuclei to another.

In our case, the microscopic current that corresponds to the intersubband transitions is a rapidly oscillating function at the frequencies of the transitions. Then, we define the polarization in such a way that its time evolution under the full Hamiltonian would lead to a microscopic current

$$\frac{d\hat{\mathbf{P}}(\mathbf{r})}{dt} = \frac{1}{i\hbar} [\hat{\mathbf{P}}(\mathbf{r}), \hat{H}] = \hat{\mathbf{j}}(\mathbf{r}). \quad (18)$$

This definition is valid in the absence of magnetic interactions. Since the polarization operator commutes with the electrical displacement field, the evolution of $\hat{\mathbf{P}}(\mathbf{r})$ is driven

only by the electronic part of Hamiltonian (17). The expression of the total current operator in the PZW gauge is

$$\hat{\mathbf{j}}(\mathbf{r}) = \frac{i\hbar e}{2m^*} [\hat{\Psi}^\dagger(\mathbf{r})\nabla_{\mathbf{r}}\hat{\Psi}(\mathbf{r}) - \nabla_{\mathbf{r}}\hat{\Psi}^\dagger(\mathbf{r})\hat{\Psi}(\mathbf{r})]. \quad (19)$$

Note that the paramagnetic term, proportional to the vector potential \mathbf{A} , is absent since in the PZW gauge the momentum of the particles is expressed as a function of their velocity only.¹⁰ Here, we have introduced the field operator $\hat{\Psi}(\mathbf{r})$, constructed from the one-particle wave functions (16):

$$\hat{\Psi}(z, \mathbf{r}_{\parallel}) = \sum_{\lambda\mathbf{k}} c_{\lambda\mathbf{k}} \phi_{\lambda}(z) \exp(i\mathbf{k}\mathbf{r}_{\parallel}) / \sqrt{S}. \quad (20)$$

Since we are interested in the intersubband transitions only, we shall consider solely the z component of the current. The latter is readily expressed as

$$\hat{j}_z(\mathbf{r}) = \frac{i\hbar e}{2Sm^*} \sum_{\lambda>\mu, \mathbf{q}} \xi_{\lambda\mu}(z) e^{i\mathbf{q}\mathbf{r}_{\parallel}} [B_{\lambda\mu\mathbf{q}} - B_{\lambda\mu-\mathbf{q}}] \quad (21)$$

with the following definitions:

$$B_{\lambda\mu\mathbf{q}}^\dagger = \sum_{\mathbf{k}} c_{\lambda\mathbf{k}+\mathbf{q}}^\dagger c_{\mu\mathbf{k}}, \quad (22)$$

$$\xi_{\lambda\mu}(z) = \phi_{\lambda}(z)\partial_z\phi_{\mu}(z) - \phi_{\mu}(z)\partial_z\phi_{\lambda}(z). \quad (23)$$

For simplicity, we have chosen the envelope wave functions of the bound states $\phi_{\lambda}(z)$ to be real. Note that the intrasubband contributions all vanish since $\xi_{\lambda\lambda}(z) = 0$ according to the above definition.

In order to establish the polarization operator in the long-wavelength limit, we first compute the commutators of the B operators (22) with the Hamiltonian (17):

$$[B_{\lambda\mu\mathbf{q}}^\dagger, \hat{H}_e] = - \sum_{\mathbf{k}} \hbar(\omega_{\lambda\mathbf{k}+\mathbf{q}} - \omega_{\mu\mathbf{k}}) c_{\lambda\mathbf{k}+\mathbf{q}}^\dagger c_{\mu\mathbf{k}}. \quad (24)$$

In the long-wavelength limit, the excitation wave vector \mathbf{q} is small compared to the typical electron wave vectors \mathbf{k} . Since we assumed parabolic bands, we can write

$$\omega_{\lambda\mathbf{k}+\mathbf{q}} - \omega_{\mu\mathbf{k}} \approx \omega_{\lambda} - \omega_{\mu} \equiv \omega_{\lambda\mu}. \quad (25)$$

Then, (24) becomes

$$[B_{\lambda\mu\mathbf{q}}^\dagger, \hat{H}_e] = -\hbar\omega_{\lambda\mu} B_{\lambda\mu\mathbf{q}}^\dagger. \quad (26)$$

This commutation relation indicates that the polarization density operator satisfying (18) is

$$\hat{P}_z(\mathbf{r}) = \frac{\hbar e}{2Sm^*} \sum_{\lambda>\mu, \mathbf{q}} \frac{\xi_{\lambda\mu}(z)}{\omega_{\lambda\mu}} e^{i\mathbf{q}\mathbf{r}_{\parallel}} [B_{\lambda\mu-\mathbf{q}}^\dagger + B_{\lambda\mu\mathbf{q}}]. \quad (27)$$

This is the expression to be used in the interaction Hamiltonian \hat{H}_{int} (3). It is clear that this expression satisfies the requirement stated in the beginning of this section. Indeed, it is a local function of space through the microscopic current density $\xi_{\lambda\mu}(z)$. The size of the confining potential enters only implicitly through the wave functions that construct $\xi_{\lambda\mu}(z)$ and we do not need to define any arbitrary averaging volume.

To express the interaction Hamiltonian \hat{H}_{int} as a function of the electronic polarization, it is convenient to split it into two parts:

$$\hat{H}_{\text{int}} = \hat{H}_{11} + \hat{H}_{12} \quad (28)$$

with \hat{H}_{11} the linear part and \hat{H}_{12} the part quadratic in the polarization. The expression of \hat{H}_{11} in the long-wavelength limit, for the case of the TM₀ mode, is readily obtained with the help of (11):

$$\hat{H}_{11} = i \sum_{\lambda>\mu, \mathbf{q}} \sqrt{\frac{\hbar\omega_{c\mathbf{q}}}{2\epsilon\epsilon_0 S L_{\text{cav}}}} e^{z_{\lambda\mu}} (a_{\mathbf{q}}^\dagger - a_{-\mathbf{q}}) (B_{\lambda\mu-\mathbf{q}}^\dagger + B_{\lambda\mu\mathbf{q}}). \quad (29)$$

Here, we have introduced the dipole matrix element $z_{\lambda\mu} = \langle \phi_{\lambda} | z | \phi_{\mu} \rangle$ of the transition $\mu \rightarrow \lambda$, and made use of the following identity:

$$\int_{-\infty}^{+\infty} \xi_{\lambda\mu}(z) dz = \frac{2m^* \omega_{\lambda\mu}}{\hbar} z_{\lambda\mu}. \quad (30)$$

This identity guarantees the equivalence between the current and dipole matrix elements, which are more commonly used in studies of intersubband transitions.^{19,25}

The quadratic term of the interaction Hamiltonian becomes

$$\hat{H}_{12} = \frac{e^2 \hbar^2}{8\epsilon\epsilon_0 S m^{*2}} \sum_{\lambda>\mu, \lambda'>\mu', \mathbf{q}} \frac{I_{\lambda\mu, \lambda'\mu'}}{\omega_{\lambda\mu} \omega_{\lambda'\mu'}} \times (B_{\lambda\mu\mathbf{q}}^\dagger + B_{\lambda\mu-\mathbf{q}}) (B_{\lambda'\mu'-\mathbf{q}}^\dagger + B_{\lambda'\mu'\mathbf{q}}), \quad (31)$$

where $I_{\lambda\mu, \lambda'\mu'}$ denotes the current-current overlap integral

$$I_{\lambda\mu, \lambda'\mu'} = \int_{-\infty}^{+\infty} \xi_{\lambda\mu}(z) \xi_{\lambda'\mu'}(z) dz. \quad (32)$$

Note that the expressions derived above are exact and general, except for the long-wavelength approximation that is satisfied for the majority of experiments with intersubband devices. For instance, they will apply for a heterostructure featuring population inversion. In the following, we are interested in the specific case of noninverted (thermalized) subbands.

III. BOSONIZED PLASMA HAMILTONIAN

A. Bright and dark states

In order to further study the interaction between the light and the thermalized subbands, we replace the fermionic Hamiltonian \hat{H}_e by an effective bosonic Hamiltonian, which contains only the polarization degrees of freedom. In this way, we obtain a fully diagonalizable Hopfield-type model. To carry out this approach, we need to replace the B operators (22) by effective bosonic operators. For this purpose, we compute the commutator

$$[B_{\lambda\mu\mathbf{q}}, B_{\lambda\mu\mathbf{q}}^\dagger] = \sum_{\mathbf{k}} (c_{\mu\mathbf{k}}^\dagger c_{\mu\mathbf{k}} - c_{\lambda\mathbf{k}+\mathbf{q}}^\dagger c_{\lambda\mathbf{k}+\mathbf{q}}) = \hat{N}_{\mu} - \hat{N}_{\lambda}. \quad (33)$$

We recognize the difference between the number operators \hat{N}_{μ} and \hat{N}_{λ} of the respective subbands. Let us define normalized operators through the relation

$$B_{\lambda\mu\mathbf{q}}^\dagger = \sqrt{\Delta N_{\lambda\mu}} b_{\lambda\mu\mathbf{q}}^\dagger \quad (34)$$

with

$$\Delta N_{\lambda\mu} = \langle \hat{N}_{\mu} \rangle - \langle \hat{N}_{\lambda} \rangle. \quad (35)$$

Here, the mean values of the operators are computed in the, say, thermal state arising from the Fermi-Dirac statistics. In the limit of weakly excited systems, the operators $b_{\lambda\mu\mathbf{q}}^\dagger$ defined above obey the bosonic commutation rules²⁶

$$[b_{\lambda\mu\mathbf{q}}, b_{\lambda\mu\mathbf{q}'}^\dagger] = \delta_{\mathbf{q},\mathbf{q}'}. \quad (36)$$

Taking into account (36), (34), and (26), we replace the fermionic Hamiltonian \hat{H}_e (17) by an effective bosonic Hamiltonian, which yields exactly the same time evolution of the weakly excited system:

$$\hat{H}'_e = \sum_{\lambda>\mu,\mathbf{q}} \hbar\omega_{\lambda\mu} b_{\lambda\mu\mathbf{q}}^\dagger b_{\lambda\mu\mathbf{q}}. \quad (37)$$

The bosonic operators introduced here describe the only intersubband excitations that couple with light,⁴ and they are therefore called ‘‘bright’’ states. To illustrate the bright states, we consider the system to be in the electric quantum limit at $T = 0$ K, where only the first subband ($\lambda = 1$) is occupied by N electrons. The fundamental state is then given by $|F\rangle = \prod_{|\mathbf{k}|<k_F} c_{1\mathbf{k}}^\dagger |0\rangle$, where k_F is the Fermi wave vector. The lowest-energy single-particle excitations can be spanned on the basis of states

$$|E_{\mathbf{k}}\rangle = c_{2\mathbf{k}}^\dagger c_{1\mathbf{k}} |F\rangle. \quad (38)$$

These basis states are eigenstates of the electronic Hamiltonian \hat{H}_e with eigenenergies $\hbar\omega_{21} + E_{\text{fond}}$, where E_{fond} is the total energy of the ground state. In the following, the energy scale is reset so that $E_{\text{fond}} = 0$. The excitations $|E_{\mathbf{k}}\rangle$ are illustrated in Fig. 3(a). For simplicity, in our example, we consider only vertical transitions $\mathbf{q} = \mathbf{0}$. The dipole moment operator \hat{d} between the subbands 1 and 2 is

$$\hat{d} = z_{12} \sum_{\mathbf{k}} (c_{2\mathbf{k}}^\dagger c_{1\mathbf{k}} + c_{1\mathbf{k}}^\dagger c_{2\mathbf{k}}). \quad (39)$$

It is easy to show that each excitation $|E_{\mathbf{k}}\rangle$ holds a dipole $z_{12} = \langle F|\hat{d}|E_{\mathbf{k}}\rangle$. We can, however, change the basis by using any appropriate linear combinations of $|E_{\mathbf{k}}\rangle$'s:

$$|B_a\rangle = \sum_{\mathbf{k}} \beta_{a,\mathbf{k}} |E_{\mathbf{k}}\rangle, \quad (40)$$

$$\sum_{\mathbf{k}} \beta_{a,\mathbf{k}} \beta_{b,\mathbf{k}}^* = \delta_{a,b}, \quad (41)$$

$$\langle F|\hat{d}|B_a\rangle = z_{12} \sum_{\mathbf{k}} \beta_{a,\mathbf{k}}. \quad (42)$$

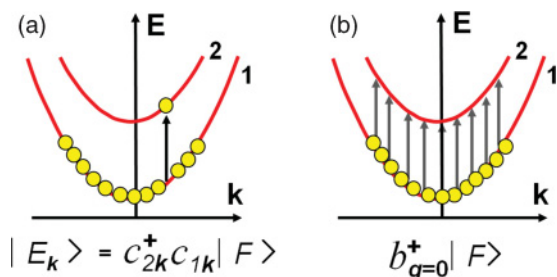


FIG. 3. (Color online) (a) One-particle excitation between two subbands. The fundamental subband is filled with N electrons at $T = 0$ K. (b) Bright excitation.

Here, $a, b = 1, \dots, N$ label the new basis states. The coefficients $\beta_{a,\mathbf{k}}$ are arbitrary within the normalization condition (41), but let us define the $a = 1$ state so that all $\beta_{1,\mathbf{k}}$ are equal. Because of (41), we then have $\beta_{1,\mathbf{k}} = 1/\sqrt{N}$ and therefore $|B_1\rangle$ is exactly the state created by the bosonic operator introduced above: $|B_1\rangle = b_{\mathbf{q}=0}^\dagger |F\rangle$. This state, which is a coherent superposition of all possible single-particle states with equal amplitudes $1/\sqrt{N}$, is illustrated in Fig. 3 (b). Next, because of (42) and (41), we have

$$\langle F|\hat{d}|B_1\rangle = z_{12}\sqrt{N}, \quad \langle F|\hat{d}|B_{a\neq 1}\rangle = 0. \quad (43)$$

These formulas express the fact that the whole oscillator strength of the system is held by the single state $b_{\mathbf{q}=0}^\dagger |F\rangle$, whereas all other $N - 1$ states, which are orthogonal to it, have a zero oscillator strength and do not couple with light.

At a first glance, it might seem that the emergence of the superradiant state $b_{\mathbf{q}=0}^\dagger |F\rangle$ is due to a mere change of the basis, and that this state does not have any particular physical meaning. Indeed, this state is perfectly degenerate with the dark states with respect to the electronic Hamiltonian \hat{H}_e . However, the inclusion of the interaction Hamiltonian (3) lifts the degeneracy between the bright superradiant state and the dark states $|B_{a\neq 1}\rangle$ since both the quadratic \hat{H}_{12} and the linear \hat{H}_{11} parts renormalize the energy of the bright state. The quadratic part \hat{H}_{12} leads to a blue-shift, as explained in the next section, and the linear part to the emergence of two polariton states. Neither \hat{H}_{11} nor \hat{H}_{12} acts on the dark states, which therefore remain at the energy of the bare intersubband transition $\hbar\omega_{21}$. These heavily degenerated dark states hinder the efficiency of the electronic injection into the polariton states.²⁷

B. Plasma Hamiltonian

The procedure of bosonization described in the previous section assigns bosonic operators $b_{\lambda\mu\mathbf{q}}$ and $b_{\lambda\mu\mathbf{q}}^\dagger$ to each intersubband transition $\mu \rightarrow \lambda$. Each transition now enters the bosonized Hamiltonian with an energy $\hbar\omega_{\lambda\mu}$. Therefore, in order to avoid cumbersome notations, from now on, we label each transition $\mu \rightarrow \lambda$ with a single Greek index α , i.e., $\alpha \equiv [\lambda, \mu]$. This means that now we count the number of excitations in the system instead of the number of subband states.

We now seek to express the interaction Hamiltonian as a function of the bosonic operators $b_{\alpha\mathbf{q}}$ and $b_{\alpha\mathbf{q}}^\dagger$. To this end, we introduce the plasma frequencies $\omega_{P\alpha}$ through the formula

$$\omega_{P\alpha}^2 = \frac{e^2 \Delta N_\alpha}{\epsilon \epsilon_0 m^* S L_{\text{eff}}^\alpha}. \quad (44)$$

Here, L_{eff}^α is the effective length introduced by Vinter and Tsui.⁷ This length is a function of the current-current correlation integral introduced by Eq. (32), and describes the spatial extension of the microscopic current density of the intersubband transition α :

$$L_{\text{eff}}^\alpha = \frac{2m^* \omega_\alpha}{\hbar} \frac{1}{I_{\alpha,\alpha}}. \quad (45)$$

We will also make use of the transition oscillator strength

$$f_{\alpha}^o = \frac{2m^*\omega_{\alpha}}{\hbar} z_{\alpha}^2. \quad (46)$$

The linear part of the interaction Hamiltonian then becomes

$$\hat{H}_{11} = i \sum_{\alpha, \mathbf{q}} \frac{\hbar \omega_{P\alpha}}{2} \sqrt{\frac{\omega_{c\mathbf{q}}}{\omega_{\alpha}}} f_{\alpha}^o f_{\alpha}^w (a_{\mathbf{q}}^{\dagger} - a_{-\mathbf{q}})(b_{\alpha-\mathbf{q}}^{\dagger} + b_{\alpha\mathbf{q}}). \quad (47)$$

Here, f_{α}^w is the overlap factor between the cavity mode and the current distribution of the transition α , defined as

$$f_{\alpha}^w = L_{\text{eff}}^{\alpha} / L_{\text{cav}}. \quad (48)$$

This definition, introduced here for simplicity for the special case of a TM_0 mode, can be generalized for a mode with an arbitrary shape, as shown in the end of this section.

We now turn to the quadratic part \hat{H}_{12} of the interaction Hamiltonian. It is expressed as a sum over pairs of transitions $\lambda > \mu, \lambda' > \mu' = \alpha, \beta$. Let us consider first the terms that correspond to the same transition $\alpha = \beta$. By combining these terms with the electronic Hamiltonian (37), we have

$$\hat{H}'_e + \hat{H}_{12}(\alpha = \beta) = \sum_{\alpha, \mathbf{q}} \left[\hbar \omega_{\alpha} b_{\alpha\mathbf{q}}^{\dagger} b_{\alpha\mathbf{q}} + \frac{\hbar \omega_{P\alpha}^2}{4\omega_{\alpha}} (b_{\alpha\mathbf{q}}^{\dagger} + b_{\alpha-\mathbf{q}})(b_{\alpha-\mathbf{q}}^{\dagger} + b_{\alpha\mathbf{q}}) \right]. \quad (49)$$

This quadratic Hamiltonian can be diagonalized with the Bogoliubov transformation²⁸ by introducing new bosonic operators $p_{\alpha\mathbf{q}}$, which satisfy

$$[p_{\alpha\mathbf{q}}, \hat{H}'_e + \hat{H}_{12}(\alpha = \beta)] = \hbar \tilde{\omega}_{\alpha} p_{\alpha\mathbf{q}}, \quad (50)$$

where $\tilde{\omega}_{\alpha}$ denotes the new eigenvalues. This diagonalization procedure yields the following results:

$$\tilde{\omega}_{\alpha} = \sqrt{\omega_{\alpha}^2 + \omega_{P\alpha}^2}, \quad (51)$$

$$p_{\alpha\mathbf{q}} = \frac{\tilde{\omega}_{\alpha} + \omega_{\alpha}}{2\sqrt{\tilde{\omega}_{\alpha}\omega_{\alpha}}} b_{\alpha\mathbf{q}} + \frac{\tilde{\omega}_{\alpha} - \omega_{\alpha}}{2\sqrt{\tilde{\omega}_{\alpha}\omega_{\alpha}}} b_{\alpha-\mathbf{q}}^{\dagger}. \quad (52)$$

In Eq. (51), the new eigenvalue $\tilde{\omega}_{\alpha}$ is exactly the frequency of the collective mode of the bidimensional electron gas known as the ‘‘intersubband plasmon.’’²² By using (44) and (52) to express the remaining $\alpha \neq \beta$ terms of \hat{H}_{12} , we arrive at the full Hamiltonian, which is now expressed in terms of the collective plasmonic operators

$$\begin{aligned} \hat{H} &= \sum_{\alpha, \mathbf{q}} \hbar \tilde{\omega}_{\alpha} p_{\alpha\mathbf{q}}^{\dagger} p_{\alpha\mathbf{q}} + \sum_{\mathbf{q}} \hbar \omega_{c\mathbf{q}} (a_{\mathbf{q}}^{\dagger} a_{\mathbf{q}} + 1/2) \\ &+ i \sum_{\alpha, \mathbf{q}} \hbar \Omega_{\alpha\mathbf{q}} (a_{\mathbf{q}}^{\dagger} - a_{-\mathbf{q}})(p_{\alpha-\mathbf{q}}^{\dagger} + p_{\alpha\mathbf{q}}) \\ &+ \sum_{\alpha \neq \beta, \mathbf{q}} \hbar \Xi_{\alpha\beta} (p_{\alpha\mathbf{q}}^{\dagger} + p_{\alpha-\mathbf{q}})(p_{\beta-\mathbf{q}}^{\dagger} + p_{\beta\mathbf{q}}). \end{aligned} \quad (53)$$

Here, we have introduced the light-matter coupling constant in the dipole gauge

$$\Omega_{\alpha\mathbf{q}} = \frac{\omega_{P\alpha}}{2} \sqrt{\frac{\omega_{c\mathbf{q}}}{\tilde{\omega}_{\alpha}}} f_{\alpha}^o f_{\alpha}^w. \quad (54)$$

The quantity $\Xi_{\alpha\beta}$ is the plasmon-plasmon coupling constant

$$\Xi_{\alpha\beta} = \frac{\omega_{P\alpha} \omega_{P\beta}}{4\sqrt{\tilde{\omega}_{\alpha}\tilde{\omega}_{\beta}}} C_{\alpha\beta}, \quad (55)$$

where the coefficient $C_{\alpha\beta}$ is the plasmon-plasmon correlation coefficient, defined as

$$C_{\alpha\beta} = \frac{I_{\alpha, \beta}}{\sqrt{I_{\alpha, \alpha} I_{\beta, \beta}}} = \frac{\int \xi_{\alpha}(z) \xi_{\beta}(z) dz}{\sqrt{I_{\alpha, \alpha} I_{\beta, \beta}}}. \quad (56)$$

The plasma Hamiltonian described in Eq. (53) is the central result of this paper. It provides a fully quantum description of the coupling between the light and the coherent collective intersubband modes of a bidimensional electron system. The Hamiltonian (53) contains both the interaction with the electromagnetic field and the coupling between plasmons from different subbands. The interplasmon coupling is contained in the coefficients $C_{\alpha\beta}$. With the definition (32), it appears simply as the normalized spatial overlap between the intersubband currents associated to the transitions α and β . This overlap vanishes when the subbands belong to spatially different quantum wells. On the contrary, $C_{\alpha\beta}$ takes values close to unity when the subbands originate from the same quantum well. The coefficients $C_{\alpha\beta}$ provide thus a convenient description for a number of cases, from spatially decoupled quantum wells (tight-binding approximation) to strongly coupled heterostructures such as a superlattice. When several intersubband plasmons are present in the system, the Bogoliubov procedure can be further applied to the interplasmon coupling terms of Eq. (53) in order to obtain the new normal modes and their coupling with the light field. These results will be presented in a separate paper.

We conclude this section by providing a very general expression of the light-matter coupling constant for an arbitrary shaped guided mode $f_{\mathbf{q}}(z)$. To establish this expression, we use the general form of the z component of the displacement field (5) instead of the special case of the TM_0 mode (11). We then express the linear coupling term \hat{H}_{11} by following the same procedure as described in Sec. II D and the beginning of this section. This leads to the result

$$\Omega_{\alpha\mathbf{q}} = \frac{\omega_{P\alpha}}{2\sqrt{\tilde{\omega}_{\alpha}}} \sqrt{\omega_{c\mathbf{q}}} \cos \theta_{\mathbf{q}} C_{\alpha, \mathbf{q}}. \quad (57)$$

Here, we have introduced the normalized current-light overlap coefficient

$$C_{\alpha, \mathbf{q}} = \frac{\int f_{\mathbf{q}}(z) \xi_{\alpha}(z) dz}{\sqrt{L_{\mathbf{q}} I_{\alpha, \alpha}}} \quad (58)$$

and the angle $\theta_{\mathbf{q}}$ is the propagation angle between the guided mode and the in-plane direction

$$\cos \theta_{\mathbf{q}} = \frac{|\mathbf{q}|c}{\sqrt{\varepsilon} \omega_{c\mathbf{q}}}. \quad (59)$$

In the previous expression, $\varepsilon = \varepsilon(z \approx z_{\alpha})$ is the background dielectric constant of the media surrounding the current density $\xi_{\alpha}(z)$. The expressions (55) and (57) reveal the striking resemblance between the plasmon-plasmon and the plasmon-light coupling constants $\Xi_{\alpha, \beta}$ and $\Omega_{\alpha, \mathbf{q}}$. Indeed, the two coupling constants are proportional to a normalized overlap factor, respectively, $C_{\alpha, \beta}$ and $C_{\alpha, \mathbf{q}}$ [Eqs. (56) and (58)]. In the same way as $C_{\alpha, \beta}$ represents the overlap integral between

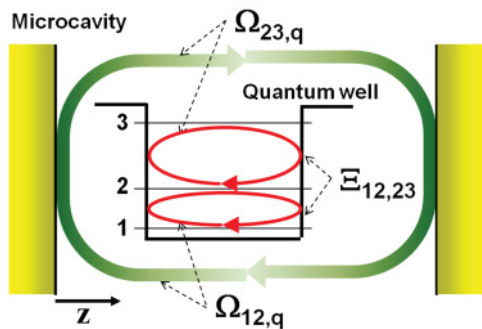


FIG. 4. (Color online) Scheme of all possible interactions between a microcavity and a three-level quantum well. The thick arrow corresponds to the electromagnetic mode and the thin arrows to the intersubband plasmon modes.

the two currents arising from transition α and β , $C_{\alpha,q}$ is the overlap between the current distribution α and the electrical field profile of the optical mode $f_q(z)$. Moreover, each plasmon enters the interaction with a weight factor $\omega_{P\alpha}/2\sqrt{\omega_\alpha}$. The weight of the light mode is $\sqrt{\omega_{cq}} \cos \theta_q$, the cosine term expressing the selection rule for intersubband transitions.¹⁹ Therefore, the interaction between the different plasmons and the interaction with the light mode have the same form in the dipole gauge. Indeed, the Hamiltonian (53) describes a set of coupled oscillators, one of which is the electromagnetic resonator, the other being the collective plasmon modes. This is schematized in Fig. 4.

In most experimental situations, the function $f_q(z)$ varies slowly at the scale of the intersubband current density $\xi_\alpha(z)$, and therefore can be taken out from the integral in Eq. (58). In this case, we recover the usual expression for the oscillator strength f_α^o (Ref. 25) using (46) and (30). This leads to the expression (54), where instead of the definition (48), we use a generalized filling factor of the form

$$f_\alpha^w = \frac{L_{\text{eff}}^\alpha f_q(z \approx z_\alpha)^2}{L_q} \cos^2 \theta_q. \quad (60)$$

[The definition (48) for the TM_0 mode is recovered by setting $\theta_q = 0$ and $L_q = L_{\text{cav}}$.] The dipole gauge provides therefore a very compact description of the interaction between the light and intersubband excitations. In particular, the simple structure of the coupling constants allows us to disclose the role played by the collective effect, described by the plasma frequencies $\omega_{P\alpha}$ and the microcavity geometry, which sets the overlap coefficients. Finally, in this formulation, the weak-coupling regime is naturally recovered for the case of vanishing plasmon-light overlap ($C_{\alpha,q} \rightarrow 0$ or $f_\alpha^w \rightarrow 0$), as expected. In this situation, which is common for absorption experiments, one measures solely the collective effects in the intersubband system contained in the matter part of the quantum Hamiltonian (53).^{7,29}

C. Case of 0D microcavities

So far, we used the expansion of the electromagnetic field into the basis of guided modes labeled by the wave vector \mathbf{q} . Our choice was motivated by the microscopic definition of the polarization density in Sec. IID, which is naturally

expanded into electronic plane waves propagating along the heterostructure slab [see, for instance, Eq. (22)].

The approach developed here allows the rigorous quantum description of 0D microcavities that confine the electromagnetic field into all three dimensions of space. Such systems have been recently employed for the study of light-matter coupling with intersubband transitions.^{6,30} In this case, the possible polarization excitations will be determined by the quantizing conditions for \mathbf{q} imposed by the microcavity boundaries.

We start by expanding the electrical displacement into laterally localized TM_0 -like modes:

$$\hat{\mathbf{D}}(\mathbf{r}) = \hat{\mathbf{D}}(z, \mathbf{r}_\parallel) = i \mathbf{e}_z \sum_m \sqrt{\frac{\varepsilon \varepsilon_0 \hbar \omega_{\text{cm}}}{2SL_{\text{cav}}}} u_m(\mathbf{r}_\parallel) (a_m^\dagger - a_m). \quad (61)$$

The index m labels the discrete cavity modes and the set of functions $u_m(\mathbf{r}_\parallel)$ describes the lateral shape of the modes. They are normalized such as

$$\iint u_m(\mathbf{r}_\parallel) u_{m'}(\mathbf{r}_\parallel) d^2 \mathbf{r}_\parallel = S \delta_{mm'}. \quad (62)$$

We must now provide the expansion of the polarization density (27) into the new basis of localized electromagnetic modes. To this end, it is very convenient to use the quantum mechanical notations $|\mathbf{q}\rangle$ and $|u_m\rangle$ so that $\langle \mathbf{r}_\parallel | \mathbf{q} \rangle = \exp(i\mathbf{q}\mathbf{r}_\parallel) / \sqrt{S}$ and $\langle \mathbf{r}_\parallel | u_m \rangle = u_m(\mathbf{r}_\parallel)$. Then, the basis transformation is expressed as

$$|u_m\rangle = \sum_{\mathbf{q}} |\mathbf{q}\rangle \langle \mathbf{q} | u_m \rangle. \quad (63)$$

Here, $\langle \mathbf{q} | u_m \rangle$ is simply the \mathbf{q} th Fourier component of the function $u_m(\mathbf{r}_\parallel)$ (Ref. 31):

$$\langle \mathbf{q} | u_m \rangle = \frac{1}{S} \iint e^{i\mathbf{q}\mathbf{r}_\parallel} u_m(\mathbf{r}_\parallel) d^2 \mathbf{r}_\parallel. \quad (64)$$

We have, accordingly, the transformation law for the B operators (22):

$$B_{\alpha m}^\dagger = \sum_{\mathbf{q}} \langle \mathbf{q} | u_m \rangle B_{\alpha \mathbf{q}}^\dagger. \quad (65)$$

Since the same transformation law applies to the bosonic operators $b_{\alpha \mathbf{q}}^\dagger$, we can readily express the expansion of the polarization density in the new basis:

$$\hat{P}_z(\mathbf{r}) = \frac{\hbar e}{2Sm^*} \sum_{\alpha, m} \frac{\sqrt{\Delta N_\alpha}}{\omega_\alpha} \xi_\alpha(z) u_m(\mathbf{r}_\parallel) [b_{\alpha m}^\dagger + b_{\alpha m}]. \quad (66)$$

The interaction Hamiltonian is also readily expressed. Details are provided in Appendix B, and the final expression for the plasma Hamiltonian of 0D microcavities is

$$\begin{aligned} \hat{H} &= \sum_{\alpha, m} \hbar \tilde{\omega}_\alpha p_{\alpha m}^\dagger p_{\alpha m} + \sum_m \hbar \omega_{\text{cm}} (a_m^\dagger a_m + 1/2) \\ &+ i \sum_{\alpha, m} \frac{\hbar \omega_{P\alpha}}{2} \sqrt{\frac{\omega_{\text{cm}}}{\omega_\alpha}} f_\alpha^o f_\alpha^w (a_m^\dagger - a_m) (p_{\alpha m}^\dagger + p_{\alpha m}) \\ &+ \sum_{\alpha \neq \beta, m} \frac{\hbar \omega_{P\alpha} \omega_{P\beta}}{4\sqrt{\omega_\alpha \omega_\beta}} C_{\alpha, \beta} (p_{\alpha m}^\dagger + p_{\alpha m}) (p_{\beta m}^\dagger + p_{\beta m}). \end{aligned} \quad (67)$$

The above Hamiltonian (67) is formally similar to the plasma Hamiltonian (53). The difference arises from the modified spectrum of electromagnetic modes, which is no longer continuum but discrete. The discrete spectrum allows us to study the simplest possible light-matter interacting system, where only the lowest intersubband transition ($\alpha = 2, 1$) interacts resonantly with a single microcavity mode that is sufficiently far from the others, say, the fundamental mode $m = 0$. Then, the plasma Hamiltonian for this polariton-dot system is reduced to⁶

$$\hat{H} = \hbar\tilde{\omega}_{21}p_{21}^\dagger p_{21} + \hbar\omega_c(a^\dagger a + 1/2) + i\frac{\hbar\omega_{P21}}{2}\sqrt{\frac{\omega_c}{\tilde{\omega}_{21}}}f_{21}^o f_{21}^w(a^\dagger - a)(p_{21}^\dagger + p_{21}). \quad (68)$$

An example of a microcavity is provided by the square patch resonators depicted in Refs. 6 and 32. In this case, the resonances are labeled by two lateral indexes $m = N, M$ and the corresponding lateral functions are

$$u_{N,M}(\mathbf{r}_{\parallel}) = \sqrt{2 - \delta_{0N}}\sqrt{2 - \delta_{0M}}\cos\left(\frac{\pi Nx}{s}\right)\cos\left(\frac{\pi My}{s}\right). \quad (69)$$

Here, s is the size of the square. The fundamental mode is actually twofold degenerate ($N = 1, M = 0$), ($N = 0, M = 1$), however, only one of the two modes can be selected in experiments with polarized light. The mode ($N = 1, M = 0$) is depicted in Fig. 5(a).

Generally, in the case of a resonant light excitation, only the spatial modes that correspond to the specific microcavity resonance will be excited. That means that the charge distribution will vibrate into well-defined spatial modes, imposed by the microcavity. The charge density $\rho(\mathbf{r})$ can be obtained from the divergence of the polarization matrix element (66), $\rho(\mathbf{r}) = \partial P_z(\mathbf{r})/\partial z$:

$$\rho_{\lambda,\mu,m}(\mathbf{r}) = \frac{e\sqrt{\Delta N_{\lambda\mu}}}{S}\phi_\lambda(z)\phi_\mu(z)u_m(\mathbf{r}_{\parallel}). \quad (70)$$

In the case of a square infinite quantum well of thickness L_{QW} , the wave functions are $\phi_\lambda(z) = \sqrt{2/L_{QW}}\sin(\lambda\pi z/L_{QW})$. The charge distribution, which cor-

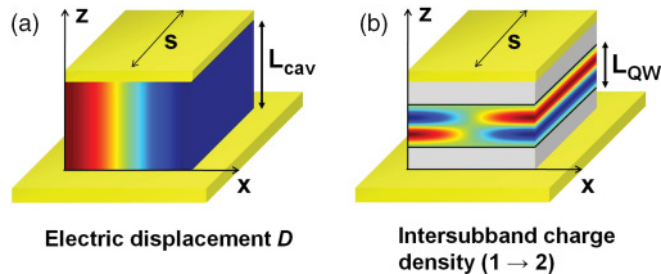


FIG. 5. (Color online) (a) Electrical displacement for the ($N = 1, M = 0$) mode of a patch microcavity with a patch size s . (b) Intersubband charge density for the fundamental transition of a quantum well with thickness L_{QW} coupled with the ($N = 1, M = 0$) mode of the microcavity.

responds to the first intersubband excitation $1 \rightarrow 2$ coupled with the fundamental cavity mode $N = 1, M = 0$, has been plotted in Fig. 5(b). This example shows how the microcavity allows us to control the spatial properties of the bright state.

D. Back transformation in the Coulomb gauge

The light-matter coupling between microcavities and intersubband transitions has been studied, so far, exclusively in the Coulomb gauge.⁴ Usually, the case of a single intersubband transition coupled with a continuum of guided modes ω_{cq} has been considered. These theoretical studies pointed out the possibility to obtain the ultrastrong-coupling regime, where the light-matter coupling constant becomes comparable to the frequency of the intersubband transition ω_{21} .⁴ In this case, the full quantum Hamiltonian, including the antiresonant terms and the quadratic vector potential term $\hat{\mathbf{A}}^2$, must be taken into account in order to describe correctly the system.⁴

In this section, we establish a link between the previous studies in the Coulomb gauge and the description in the dipole gauge developed here. We shall consider the case of a single intersubband transition ($\lambda = 2, \mu = 1$), coupled with the TM_0 mode. We then perform a unitary transformation to the Hamiltonian in order to obtain its expression in the Coulomb gauge. The transformed Hamiltonian will have identical eigenvalues as the original one, but will be expressed in terms of the vector and scalar potentials \mathbf{A} and V .

In this section, it is convenient to keep the individual subband indexes 2, 1. We return to the form of the Hamiltonian with a single intersubband transition before the Bogoliubov transformation leading to the depolarization shift

$$\hat{H} = \sum_{\mathbf{q}} \hbar\omega_{21}b_{\mathbf{q}}^\dagger b_{\mathbf{q}} + \sum_{\mathbf{q}} \hbar\omega_{cq}(a_{\mathbf{q}}^\dagger a_{\mathbf{q}} + 1/2) + i\sum_{\mathbf{q}} \frac{\hbar\omega_P}{2}\sqrt{\frac{\omega_{cq}}{\omega_{21}}}f_{21}^o f_{21}^w(a_{\mathbf{q}}^\dagger - a_{-\mathbf{q}})(b_{-\mathbf{q}}^\dagger + b_{\mathbf{q}}) + \frac{\hbar\omega_P^2}{4\omega_{21}}(b_{\mathbf{q}}^\dagger + b_{-\mathbf{q}})(b_{-\mathbf{q}}^\dagger + b_{\mathbf{q}}). \quad (71)$$

(The subscripts “21” have been dropped for operators.) The vector potential for the TM_0 mode is

$$\hat{\mathbf{A}}(\mathbf{r}) = \mathbf{e}_z \sum_{\mathbf{q}} \sqrt{\frac{\hbar}{2\epsilon\epsilon_0 S L_{cav}\omega_{cq}}} e^{i\mathbf{q}\mathbf{r}_{\parallel}} (a_{\mathbf{q}} + a_{-\mathbf{q}}^\dagger). \quad (72)$$

We use (72) to express the inverse PZW unitary transformation¹

$$T = \exp\left(-\frac{i}{\hbar} \int \hat{\mathbf{A}}(\mathbf{r}) \cdot \hat{\mathbf{P}}(\mathbf{r}) d^3\mathbf{r}\right). \quad (73)$$

It is written in the case of a single intersubband transition as

$$T = \exp\left(-i \sum_{\mathbf{q}} \chi_{\mathbf{q}}(a_{\mathbf{q}}^\dagger + a_{-\mathbf{q}})(b_{-\mathbf{q}}^\dagger + b_{\mathbf{q}})\right), \quad (74)$$

$$\chi_{\mathbf{q}} = \frac{1}{2}\sqrt{\frac{\omega_P^2 f_{21}^o f_{21}^w}{\omega_{21}\omega_{cq}}}. \quad (75)$$

Recalling the parity of the photon dispersion $\omega_{c\mathbf{q}} = \omega_{c-\mathbf{q}}$, the following transformation laws of the bosonic operators are obtained:

$$T^+ b_{\mathbf{q}} T = b_{\mathbf{q}} - i\chi_{\mathbf{q}}(a_{-\mathbf{q}}^\dagger + a_{\mathbf{q}}), \quad (76)$$

$$T^+ a_{\mathbf{q}} T = a_{\mathbf{q}} - i\chi_{\mathbf{q}}(b_{-\mathbf{q}}^\dagger + b_{\mathbf{q}}). \quad (77)$$

With these relations and their Hermitian conjugates, the transformed Hamiltonian is obtained to be

$$\begin{aligned} T^+ \hat{H} T &= \sum_{\mathbf{q}} \hbar\omega_{21} b_{\mathbf{q}}^\dagger b_{\mathbf{q}} + \sum_{\mathbf{q}} \hbar\omega_{c\mathbf{q}}(a_{\mathbf{q}}^\dagger a_{\mathbf{q}} + 1/2) \\ &+ i \sum_{\mathbf{q}} \hbar\bar{\Omega}_{\mathbf{q}}(a_{\mathbf{q}}^\dagger + a_{-\mathbf{q}})(b_{\mathbf{q}} - b_{-\mathbf{q}}^\dagger) \\ &+ \sum_{\mathbf{q}} \frac{\hbar\bar{\Omega}_{\mathbf{q}}^2}{\omega_{12}}(a_{\mathbf{q}}^\dagger + a_{-\mathbf{q}})(a_{-\mathbf{q}}^\dagger + a_{\mathbf{q}}) \\ &+ (1 - f_{21}^o f_{21}^w) \sum_{\mathbf{q}} \frac{\hbar\omega_P^2}{4\omega_{21}}(b_{\mathbf{q}}^\dagger + b_{-\mathbf{q}})(b_{-\mathbf{q}}^\dagger + b_{\mathbf{q}}). \end{aligned} \quad (78)$$

Here, $\bar{\Omega}_{\mathbf{q}}$ is the light-matter coupling constant in the minimal coupling gauge

$$\bar{\Omega}_{\mathbf{q}} = \omega_{21} \chi_{\mathbf{q}} = \frac{\omega_P}{2} \sqrt{\frac{\omega_{21}}{\omega_{c\mathbf{q}}} f_{21}^o f_{21}^w}. \quad (79)$$

The first four terms of (78), together with (79), provide the Hopfield-type Hamiltonian used for the theoretical study of intersubband polaritons.^{4,33} Namely, the presence of the $\hat{\mathbf{A}}^2$ term and the antiresonant terms leads to the ultrastrong-coupling regime.⁴ The latter has been defined as the situation where the coupling term $\bar{\Omega}_{\mathbf{q}}$, taken at resonance $\omega_{21} = \omega_{c\mathbf{q}}$, becomes comparable with the energy of the intersubband transition ω_{21} :

$$\bar{\Omega}_{\mathbf{q}}(\omega_{21} = \omega_{c\mathbf{q}}) = \frac{\omega_P}{2} \sqrt{f_{21}^o f_{21}^w} \approx \omega_{21}. \quad (80)$$

Since from (78) and (79) the $\hat{\mathbf{A}}^2$ term is proportional to the square of the plasma frequency ω_P^2 , we see that the ultrastrong-coupling regime, as defined in Ref. 4, is obtained in systems featuring high photonic confinement factor f_{21}^w , and high plasma frequency ω_P , i.e., high electronic densities. However, for high electronic densities, the Coulomb interaction brings important dynamical corrections.⁸ The latter are already present in the dipole gauge, which naturally includes the collective excitations of the electron gas, as described in Sec. III B. In the Hamiltonian (78) expressed in the Coulomb gauge, these corrections actually arise from the last term. In Appendix C, we show that this term can indeed be cast in a form of a long-wavelength limit of the Coulomb potential.

The Coulomb correction in the Hamiltonian (78) contains an interesting new element, which is the geometrical prefactor $(1 - f_{21}^o f_{21}^w)$. This prefactor is equal to one in the case of a very large cavity ($f_{21}^w \rightarrow 0$). This case of vanishing photon confinement corresponds, for instance, to the multipass wave guides employed for the absorption measurements where the depolarization shift is observed. However, the confinement factor $f_{21}^o f_{21}^w$ becomes an important correction in the case of microcavities with filling factors f_{21}^w close to unity, such as

the double-metal microcavities.^{6,11,30} We interpret the factor $-f_{21}^o f_{21}^w$ as an image contribution to the Coulomb interaction due to the boundary conditions of the electric field at the microcavity walls. In other words, it can be seen as a local field correction due to the partial screening of the microcavity field by the oscillating intersubband charges. Indeed, both the displacement field $\hat{\mathbf{D}}_z(\mathbf{r})$ and the polarization field $\hat{\mathbf{P}}_z(\mathbf{r})$ that we used to construct the PZW Hamiltonian satisfy the boundary conditions on the cavity walls, which are transported to the Coulomb correction through the unitary transformation (74).

Note that the unitary transformation (74) holds only for a truncated Hilbert space, where we retained only the first intersubband transition and the fundamental waveguide mode. The full gauge equivalence is established correctly only if the complete set of quantum transitions and electromagnetic modes of the system are accounted for.³⁴ This issue will be discussed elsewhere.

We can combine the last term in the Hamiltonian (78) with the first one, and perform a Bogoliubov diagonalization just like in Sec. III B. As a result, we obtain a renormalized intersubband frequency with an effective depolarization shift, which takes into account the local field corrections, contained in the factor $f_{21}^o f_{21}^w$:

$$\bar{\omega}_{21} = \sqrt{\omega_{21}^2 + \omega_P^2(1 - f_{21}^o f_{21}^w)}. \quad (81)$$

The local field factor $1 - f_{21}^o f_{21}^w$ yields an effective plasma frequency $\omega_P \sqrt{1 - f_{21}^o f_{21}^w}$. We can then rewrite the full Hamiltonian in the Coulomb gauge (78) using Eq. (81) and the corresponding polarization operators. The result is exactly the Hamiltonian of Ref. 4, used for the study of the ultrastrong-coupling regime, where the bare intersubband frequency has been replaced by the effective frequency $\bar{\omega}_{21}$:

$$\begin{aligned} T^+ \hat{H} T &= \sum_{\mathbf{q}} \hbar\bar{\omega}_{21} b_{\mathbf{q}}^\dagger b_{\mathbf{q}} + \sum_{\mathbf{q}} \hbar\omega_{c\mathbf{q}}(a_{\mathbf{q}}^\dagger a_{\mathbf{q}} + 1/2) \\ &+ i \sum_{\mathbf{q}} \hbar\bar{\Omega}_{\mathbf{q}}(a_{\mathbf{q}}^\dagger + a_{-\mathbf{q}})(b_{\mathbf{q}} - b_{-\mathbf{q}}^\dagger) \\ &+ \sum_{\mathbf{q}} \frac{\hbar\bar{\Omega}_{\mathbf{q}}^2}{\bar{\omega}_{21}}(a_{\mathbf{q}}^\dagger + a_{-\mathbf{q}})(a_{-\mathbf{q}}^\dagger + a_{\mathbf{q}}). \end{aligned} \quad (82)$$

Note that now $b_{\mathbf{q}}$ describes the bosonic operator after the Bogoliubov transformation, and the frequency $\bar{\omega}_{21}$ should be used in the definition of $\bar{\Omega}_{\mathbf{q}}$. This result validates the studies performed in the Coulomb gauge,³⁵ in the limit of microcavities with large filling factors, where $\bar{\omega}_{21} \approx \omega_{21}$. However, contrary to Refs. 4 and 35, the effective Hamiltonian (82) includes also the correct limit of the weak-coupling regime, obtained for vanishing overlap with the cavity mode $f_{21}^w \rightarrow 0$. In this case, from expression (81), we recover the renormalized transition frequency $\bar{\omega}_{21}$, whereas the Hamiltonians in Refs. 4 and 35 would predict only the bare intersubband spacing ω_{21} .

IV. PROPERTIES OF THE POLARITON STATES

A. Polariton dispersion

We now analyze coupled light-matter polariton states arising from the dipolar Hamiltonian. To simplify, we ignore the coupling between plasmons on different subbands. This is

equivalent to consider a single intersubband transition ω_α , not necessarily the fundamental one, in interaction with the TM_0 mode. All the results that will be stated remain also valid for 0D resonators. The corresponding plasma Hamiltonian is

$$\hat{H} = \sum_{\mathbf{q}} \hbar \tilde{\omega}_\alpha p_{\mathbf{q}}^\dagger p_{\mathbf{q}} + \sum_{\mathbf{q}} \hbar \omega_{c\mathbf{q}} (a_{\mathbf{q}}^\dagger a_{\mathbf{q}} + 1/2) + i \sum_{\mathbf{q}} \frac{\hbar \omega_{p\alpha}}{2} \sqrt{\frac{\omega_{c\mathbf{q}}}{\tilde{\omega}_\alpha}} f_\alpha^o f_\alpha^w (a_{\mathbf{q}}^\dagger - a_{-\mathbf{q}}) (p_{-\mathbf{q}}^\dagger + p_{\mathbf{q}}). \quad (83)$$

This Hamiltonian is very similar to a Dicke model.³⁶ However, the coupling coefficient is proportional to $\omega_p/\sqrt{\tilde{\omega}_\alpha}$ and has a nonlinear dependence on ω_p because of the formula of the depolarization shift $\tilde{\omega}_\alpha = \sqrt{\omega_\alpha^2 + \omega_p^2}$. We show further that this nonlinearity leads to the no-go theorem for quantum well systems, and the Hamiltonian (83) does not allow a quantum phase transition.¹³ The Hamiltonian (83) can be diagonalized exactly by introducing the polariton operator

$$\Pi_{\mathbf{q}} = x_{\mathbf{q}} a_{\mathbf{q}} + y_{\mathbf{q}} a_{-\mathbf{q}}^\dagger + z_{\mathbf{q}} p_{\mathbf{q}} + t_{\mathbf{q}} p_{-\mathbf{q}}^\dagger. \quad (84)$$

The Hopfield coefficients introduced here satisfy the normalization condition

$$|x_{\mathbf{q}}|^2 - |y_{\mathbf{q}}|^2 + |z_{\mathbf{q}}|^2 - |t_{\mathbf{q}}|^2 = 1. \quad (85)$$

The Hopfield-Bogoliubov determinant corresponding to the equation $[\hat{H}, \Pi_{\mathbf{q}}] = \hbar \omega_{\mathbf{q}} \Pi_{\mathbf{q}}$ is then

$$\begin{vmatrix} \omega_{c\mathbf{q}} - \omega_{\mathbf{q}} & 0 & i\Omega_{\mathbf{q}} & i\Omega_{\mathbf{q}} \\ 0 & -\omega_{c\mathbf{q}} - \omega_{\mathbf{q}} & i\Omega_{\mathbf{q}} & i\Omega_{\mathbf{q}} \\ -i\Omega_{\mathbf{q}} & i\Omega_{\mathbf{q}} & \tilde{\omega}_\alpha - \omega_{\mathbf{q}} & 0 \\ i\Omega_{\mathbf{q}} & -i\Omega_{\mathbf{q}} & 0 & -\tilde{\omega}_\alpha - \omega_{\mathbf{q}} \end{vmatrix} \quad (86)$$

with $\Omega_{\mathbf{q}}$ the light-matter coupling constant from (54) (the subscript α has been dropped). Zeroing the determinant (86) provides the eigenvalue equation

$$(\omega_{\mathbf{q}}^2 - \tilde{\omega}_\alpha^2)(\omega_{\mathbf{q}}^2 - \omega_{c\mathbf{q}}^2) = f_\alpha^o f_\alpha^w \omega_{p\alpha}^2 \omega_{c\mathbf{q}}^2. \quad (87)$$

This biquadratic equation can be solved analytically, the two real solutions $\omega_{\mathbf{q},+}$ and $\omega_{\mathbf{q},-}$ being the frequencies of the two coupled states. The Hopfield coefficients are also readily expressed in closed form. For instance, we can define a photonic part $h_p = |x_{\mathbf{q}}|^2 - |y_{\mathbf{q}}|^2$ and an electronic part $h_e = |z_{\mathbf{q}}|^2 - |t_{\mathbf{q}}|^2$ linked by the relation $h_p + h_e = 1$. For the photonic part, we obtain the expressions

$$h_{p,+} = \frac{\omega_{\mathbf{q},+}^2 - \tilde{\omega}_\alpha^2}{\omega_{\mathbf{q},+}^2 - \omega_{\mathbf{q},-}^2}, \quad h_{p,-} = \frac{\tilde{\omega}_\alpha^2 - \omega_{\mathbf{q},-}^2}{\omega_{\mathbf{q},+}^2 - \omega_{\mathbf{q},-}^2}. \quad (88)$$

Note that we have necessarily $h_{p,+} + h_{p,-} = 1$ (and therefore $h_{e,+} + h_{e,-} = 1$).

The polariton frequencies $\omega_{\mathbf{q},\pm}$, as well as the electronic Hopfield coefficients $h_{e,\pm}$ have been plotted as a function of the cavity frequency $\omega_{c\mathbf{q}}$ on Figs. 6(a) and 6(c). For this illustration, we have used the numerical values $\omega_p = 0.83\omega_\alpha$, $f_\alpha^o = 1$, and $f_\alpha^w = 0.8$. As seen from Fig. 6(a), the polariton dispersion features a gap. The upper edge of the gap, obtained at $\omega_{c\mathbf{q}} = 0$, is the frequency of the intersubband plasmon $\tilde{\omega}_\alpha$. The lower edge is easily estimated from Eq. (87) to be

$$\omega_{\mathbf{q},-}|_{\omega_{c\mathbf{q}} \rightarrow \infty} = \sqrt{\omega_\alpha^2 + \omega_{p\alpha}^2 (1 - f_\alpha^o f_\alpha^w)} = \bar{\omega}_\alpha. \quad (89)$$

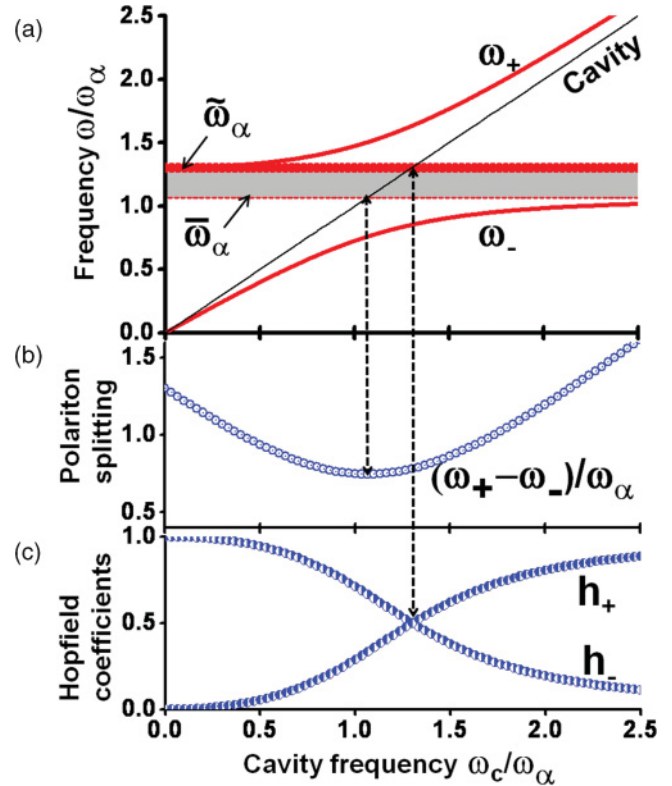


FIG. 6. (Color online) (a) Polariton dispersion, normalized at the bare intersubband transition ω_α . (b) Splitting of the two polariton states. (c) Hopfield coefficients. In these figures, the subscript \mathbf{q} has been dropped for clarity. The numerical values used for solving Eq. (87) are $\omega_p = 0.83\omega_\alpha$, $f_\alpha^o = 1$, and $f_\alpha^w = 0.8$.

In the next section, we show that $f_\alpha^o f_\alpha^w < 1$; therefore, the lower gap edge always appears at a frequency higher than the bare intersubband frequency ω_α . The impossibility for the light to propagate at the gap energies can be explained by the destructive interference between the microcavity electromagnetic field and the local field created by the collective electronic oscillations.

The most important aspect of the strong-light-matter-coupling regime is the mixing between the electronic and photonic degrees of freedom. This mixing is quantified by the Hopfield coefficients (88). Namely, the coupled system features maximum mixing when the photonic part of the Hopfield coefficients equals the electronic part: $h_{e,\pm} = h_{p,\pm} = 1/2$. From Eq. (88), we readily obtain that this is satisfied when the cavity is tuned into resonance with the intersubband plasmon:

$$h_{e,\pm} = h_{p,\pm} \Leftrightarrow \omega_{c\mathbf{q}} = \tilde{\omega}_\alpha. \quad (90)$$

This has been illustrated in Fig. 6(c). In the well-known Jaynes-Cummings model,³⁷ the maximum mixing also corresponds to the point of minimal splitting $\omega_{\mathbf{q},+} - \omega_{\mathbf{q},-}$ between the two polariton states. However, this is not true in the general case. As shown in Appendix D, the minimum splitting occurs when the cavity is resonant with the lower gap-edge frequency [Eq. (89)]

$$\frac{d(\omega_{\mathbf{q},+} - \omega_{\mathbf{q},-})}{d\omega_{c\mathbf{q}}} = 0 \Leftrightarrow \omega_{c\mathbf{q}} = \bar{\omega}_\alpha. \quad (91)$$

This is also illustrated in Fig. 6(b). Moreover, in Appendix D, we show that the minimal splitting can be computed exactly, and the result is

$$\min(\omega_{q,+} - \omega_{q,-}) = \sqrt{f_{\alpha}^o f_{\alpha}^w} \omega_P = 2\Omega_R. \quad (92)$$

We recognize the quantity $2\Omega_R$ to be the Rabi splitting, as known from the usual definition³⁸

$$2\Omega_R = \sqrt{\frac{f_{\alpha}^o e^2 (\Delta N_{\alpha} / S)}{\epsilon \epsilon_0 m^* L_{\text{cav}}}}. \quad (93)$$

Note that this is an exact result, which is valid for all orders of light-matter interaction. A more general result for an arbitrary cavity can be obtained with the expressions (57) or (60). The quantity $2\Omega_R$ can therefore be used as an experimental measure of the interaction strength, even in the ultrastrong-coupling regime.

We see that both edges of the gap $\bar{\omega}_{\alpha}$ and $\tilde{\omega}_{\alpha}$ play an important role in the theory. The frequency $\tilde{\omega}_{\alpha}$ defines the point of maximum quantum mixing, whereas $\bar{\omega}_{\alpha}$ defines the point of minimum splitting $2\Omega_R$. However, we can observe from the plot on Fig. 6(b) that the splitting around the point $\omega_{c,q} = \tilde{\omega}_{\alpha}$ is not very different from $2\Omega_R$. This feature is a characteristic of the ultrastrong-coupling regime, where we can no longer define a strict resonance condition for the optimal coupling point. Indeed, the system will feature almost identical coupling energy $2\hbar\Omega_R$ if the cavity resonates with any frequency in the band between $\bar{\omega}_{\alpha}$ and $\tilde{\omega}_{\alpha}$. The three characteristic frequencies $\tilde{\omega}_{\alpha}$, $\bar{\omega}_{\alpha}$, and $2\Omega_R$ are linked through the simple relation

$$\tilde{\omega}_{\alpha}^2 = \bar{\omega}_{\alpha}^2 + 4\Omega_R^2. \quad (94)$$

As pointed out in Ref. 4, for a very large interaction strength, the effects of the quadratic and antiresonant terms in the interaction Hamiltonian become important. These effects are manifested with the nonlinear behavior of the polariton frequencies $\omega_{q,\pm}$ as a function of the Rabi splitting $2\Omega_R$.⁴ Since the light-matter interaction strength scales as the plasma frequency ω_P [Eqs. (92) and (93)], we have studied these effects as a function of ω_P , as shown in Fig. 7. Experimentally, ω_P can be varied either through the temperature of the system or by applying a gate voltage.³⁹ In both cases, one controls the subband population difference ΔN_{α} . For the plot of Fig. 7, we

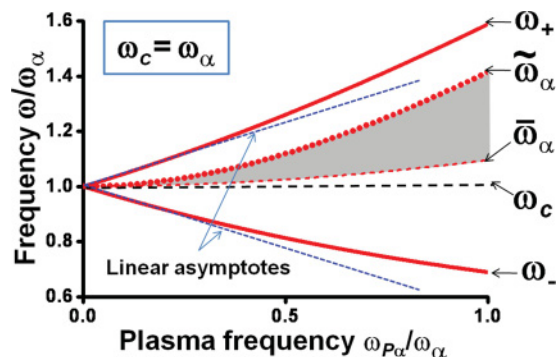


FIG. 7. (Color online) Polariton frequencies as a function of the plasma frequency for a cavity resonant with the bare intersubband transition $\omega_{c,q} = \omega_{\alpha}$. The gray area indicates the gap. For this figure, we have used $f_{\alpha}^o = 1$ and $f_{\alpha}^w = 0.8$. The linear asymptotes correspond to the Jaynes-Cummings model.

have chosen a cavity that is resonant with the bare intersubband transition when $\omega_P = 0$, i.e., $\omega_{c,q} = \omega_{\alpha}$. Moreover, in this example, we neglect the Hartree correction of the bare intersubband frequency as the number of charges in the system progressively increases. This assumption is true for a sufficiently thin square quantum well. Because both frequencies $\bar{\omega}_{\alpha}$ and $\tilde{\omega}_{\alpha}$ increase with ω_P due to the depolarization effect, the system gets blue-shifted from the cavity mode, however, the blue-shift is much smaller for $\bar{\omega}_{\alpha}$. The Jaynes-Cummings model corresponds to the linear asymptotes of the polariton branches at low ω_P . Figure 7 clearly shows that this model ceases to be valid for high electronic densities. Moreover, the magnitude of the polariton gap increases as the polariton branches depart from the linear asymptotes. Therefore, the measurement of the gap can be considered as a direct spectroscopic evidence of the ultrastrong-coupling regime.^{6,11}

Along with the charge density, the second ingredient of the light-matter interaction is the overlap factor f_{α}^w between the photonic mode and the intersubband current. As evident from the expression of the Hamiltonian in the Coulomb gauge (78), this factor controls not only the intensity of the light-matter coupling [linear term in Eq. (78)], but also the relative weight between the longitudinal Coulomb corrections [last term in (78)] and the transverse corrections contained in the \mathbf{A}^2 term.

The influence of the overlap factor f_{α}^w on the polariton dispersion is illustrated in Fig. 8. In this plot, the cavity frequency $\omega_{c,q}$ is slightly blue-shifted with respect to the bare intersubband transition ω_{α} . When $f_{\alpha}^w = 0$, we recover two uncoupled oscillators at frequencies $\omega_{c,q}$ and $\tilde{\omega}_{\alpha}$ as expected from Eq. (87). For small values of f_{α}^w , there is a small splitting that appears when the cavity is tuned with the intersubband plasmon $\omega_{c,q} = \tilde{\omega}_{\alpha}$. In this case, the \mathbf{A}^2 term of the Hamiltonian (78), which scales as $(f_{\alpha}^w)^2$, is negligible. The polariton gap is also negligible since $\bar{\omega}_{\alpha} \approx \tilde{\omega}_{\alpha}$, and the system is described by the Jaynes-Cummings model with a resonant frequency $\tilde{\omega}_{\alpha}$ renormalized by the Coulomb interactions.

On the contrary, for filling factors close to one ($f_{\alpha}^w \approx 1$), the Coulomb correction in the Hamiltonian (78) is negligible, and the weight of the quadratic term shifts to \mathbf{A}^2 . If the electronic

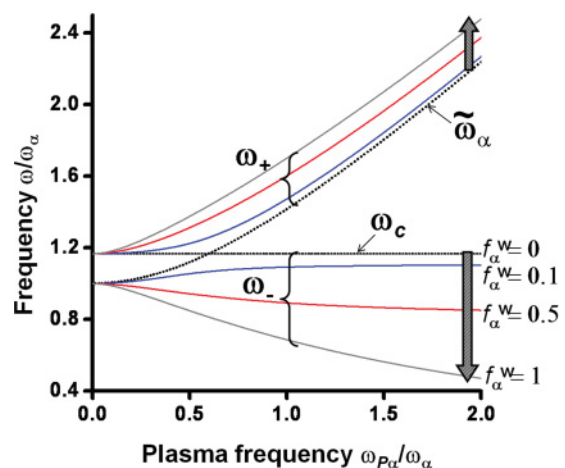


FIG. 8. (Color online) Illustration of the polariton frequencies for cavities with increasing filling factor f_{α}^w . For this illustration, the cavity is slightly blue-shifted with respect to the bare intersubband frequency ω_{α} .

density is sufficiently high, the system enters the ultrastrong-coupling regime as defined in Ref. 4. The resonance condition $\omega_{c\mathbf{q}} = \tilde{\omega}_\alpha$ loses its strict meaning, as the cavity can be resonant with any frequency in the polariton gap.

B. No-go theorem

The no-go theorem states the impossibility of the lower polariton state to acquire zero energy when the light-matter interaction is increased.¹² This property is related to the quadratic term of the interaction light-matter Hamiltonian. For intersubband polaritons, the no-go theorem becomes particularly clear in the dipole gauge, where, as shown below, it stems from the depolarization effect.

The asymptotic value of the lower polariton frequency for very high plasma frequencies $\omega_{P\alpha} \rightarrow \infty$ is deduced from Eq. (87):

$$\omega_-^2 |_{\omega_{P\alpha} \rightarrow \infty} \rightarrow \omega_{c\mathbf{q}}^2 (1 - f_\alpha^w f_\alpha^o). \quad (95)$$

Note that this limit does not contain the bare intersubband frequency ω_α , and therefore is independent from the eventual Hartree corrections to the heterostructure potential. The no-go theorem for intersubband polariton is then equivalent to the following strict inequality:

$$f_\alpha^w f_\alpha^o < 1. \quad (96)$$

This inequality can be proven by using the properties of the intersubband current matrix element $\xi_\alpha(z)$ (23), which allows us to express the overlap factor $f_\alpha^w = L_{\text{eff}}^\alpha / L_{\text{cav}}$ through Eq. (45):

$$f_\alpha^w = \frac{2m^* \omega_\alpha}{\hbar L_{\text{cav}}} \frac{1}{\int_{-\infty}^{\infty} \xi_\alpha^2(z) dz}. \quad (97)$$

We suppose that wave functions of the bound states and their derivatives decay sufficiently fast, so that $\xi_\alpha(z)$ is zero close to the cavity boundaries, as illustrated in Fig. 9. Then, we can define a domain with a finite size $L_{\text{QW}} < L_{\text{cav}}$, which we can arbitrarily call ‘‘quantum well’’ such as all the wave functions and their derivatives are zero outside this domain (Fig. 9). We chose the origin of the coordinates so that $0 \leq z \leq L_{\text{QW}}$ inside the quantum well. We then reexpress the

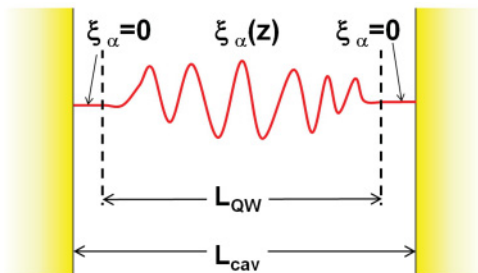


FIG. 9. (Color online) Sketch of the intersubband current $\xi_\alpha(z)$ for a heterostructure in a cavity with thickness L_{cav} . We suppose that the current decays sufficiently fast so it can be considered as null close to the cavity boundaries. We can then define a region of space with a thickness $L_{\text{QW}} < L_{\text{cav}}$ containing the entire current density.

current-current integral in the nonlocal form

$$\int_{-\infty}^{+\infty} \xi_\alpha(z)^2 dz = \iint_{-\infty}^{+\infty} \xi_\alpha(z) \xi_\alpha(z') \delta(z - z') dz dz'. \quad (98)$$

We can choose an arbitrary orthogonal basis of real functions $\chi_n(z)$ on the segment $[0, L_{\text{QW}}]$ in order to span the delta function:

$$\delta(z - z') = \sum_n \chi_n(z) \chi_n(z'). \quad (99)$$

This basis is not necessarily the basis of envelope wave functions. The expansion of the integral (98) on the basis $\chi_n(z)$ is

$$\int_{-\infty}^{+\infty} \xi_\alpha(z)^2 dz = \sum_n \left(\int_0^{L_{\text{QW}}} \xi_\alpha(z) \chi_n(z) dz \right)^2. \quad (100)$$

An evident choice for $\chi_n(z)$ is the Fourier basis on the segment $[0, L_{\text{QW}}]$

$$\chi_n(z) = \begin{cases} \sqrt{\frac{2 - \delta_{0,n}}{L_{\text{QW}}}} \cos\left(\frac{2\pi n z}{L_{\text{QW}}}\right) & n \text{ even,} \\ \sqrt{\frac{2}{L_{\text{QW}}}} \sin\left(\frac{2\pi n z}{L_{\text{QW}}}\right) & n \text{ odd.} \end{cases} \quad (101)$$

With this particular choice, the first basis function $\chi_0(z) = \sqrt{1/L_{\text{QW}}}$ is constant on the segment $[0, L_{\text{QW}}]$. Since all terms of Eq. (100) are positive, we have the Cauchy-Schwartz inequality for the current-current overlap:

$$\int_{-\infty}^{+\infty} \xi_\alpha(z)^2 dz > \frac{1}{L_{\text{QW}}} \left(\int_0^{L_{\text{QW}}} \xi_\alpha(z) dz \right)^2. \quad (102)$$

The right-hand side of the last equation can be expressed with the oscillator strength according to the identities (30) and (46). By combining this expression with the definition (97), we obtain the following inequality:

$$L_{\text{eff}}^\alpha < \frac{L_{\text{QW}}}{f_\alpha^o}. \quad (103)$$

This result shows that the higher the oscillator strength of an intersubband transition, the more the corresponding current density is localized in the space. This provides directly the no-go theorem since it leads to the inequality

$$f_\alpha^w f_\alpha^o < \frac{L_{\text{QW}}}{L_{\text{cav}}} < 1. \quad (104)$$

Therefore, the no-go theorem is a consequence of the confinement of the electronic plasma in a finite volume of space.¹³ This confinement is also the origin of the depolarization shift, which arises from the plasma energy of the bound charges.

The inequality (103) provides a lower bound for the plasma energy of the system. The plasma energy is quantified as the weight of the $\hat{\mathbf{P}}^2$ term in the plasma Hamiltonian (49):

$$\hbar \frac{\omega_{P\alpha}^2}{4\omega_\alpha} = \frac{\hbar e^2}{\varepsilon \varepsilon_0 m^* \omega_\alpha} \times \frac{\Delta N_\alpha}{4SL_{\text{eff}}^\alpha}. \quad (105)$$

By using the inequality (103) and the definition of the oscillator strength (46), we obtain the following inequality for the plasma energy:

$$\hbar \frac{\omega_{P\alpha}^2}{4\omega_\alpha} > \frac{d_\alpha^2}{2\varepsilon \varepsilon_0} \times \frac{\Delta N_\alpha}{SL_{\text{QW}}}. \quad (106)$$

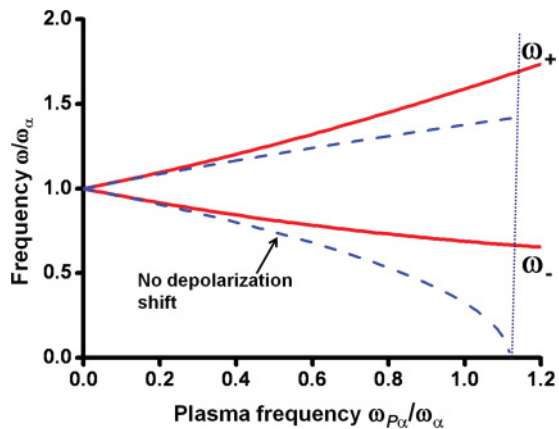


FIG. 10. (Color online) Comparison of the polariton dispersion, at resonance ($\omega_{cq} = \omega_\alpha$), with and without the depolarization effect. For simplicity, the Hartree shift of ω_α is neglected in this illustration.

Here, $d_\alpha = ez_\alpha$ is the dipole moment of the intersubband transition. The left side of (106) corresponds exactly to the classical self-interaction energy of ΔN_α dipoles uniformly distributed in a volume SL_{QW} .¹⁰ According to Eq. (106), the quantum self-energy is higher than the classical one since the wave functions of the bound states illustrated in Fig. 2 provide stronger spatial confinement of the charged particles.

The plasma energy of the charged particles localized in a finite volume compensates for the energy decrease of the lower polariton as the light-matter-coupling strength is increased. This is illustrated in Fig. 10, where we have compared the polariton branches ω_\pm as a function of ω_P with the solution of Eq. (87) when the depolarization shift is discarded, i.e., when $\tilde{\omega}_\alpha$ is replaced with ω_α . The cavity is chosen so that $\omega_{cq} = \omega_\alpha$, and the Hartree corrections have been neglected for clarity. It is clearly seen that the depolarization effect prevents the lower polariton energy to reach zero, which is an equivalent statement of the no-go theorem for intersubband transitions.

C. Effective dielectric function

The dispersion relation (87) allows us to obtain the effective dielectric constant $\varepsilon_{\text{eff}}(\omega)$ of the polaritonic medium. The latter can be defined through the propagation equation

$$\varepsilon_{\text{eff}}(\omega_{\mathbf{q}}) \frac{\omega_{\mathbf{q}}^2}{c^2} = \mathbf{q}^2. \quad (107)$$

Since for the TM_0 mode $\omega_{cq}^2 = c^2 \mathbf{q}^2 / \varepsilon$, we obtain from (87)

$$\frac{\varepsilon}{\varepsilon_{\text{eff}}(\omega)} = 1 + \frac{f_\alpha^o f_\alpha^w \omega_{P\alpha}^2}{\omega^2 - \tilde{\omega}_\alpha^2}. \quad (108)$$

Note that the zero of the dielectric constant $\varepsilon_{\text{eff}}(\omega)$ corresponds to the frequency of the intersubband plasmon $\tilde{\omega}_\alpha$, as expected. The above expression can be recast in the form

$$\frac{\varepsilon}{\varepsilon_{\text{eff}}(\omega)} = \frac{1 - f_\alpha^o f_\alpha^w}{\varepsilon} + \frac{f_\alpha^o f_\alpha^w}{\varepsilon_{QW}(\omega)}, \quad (109)$$

where $\varepsilon_{QW}(\omega)$ is the dielectric constant of the heterostructure alone:

$$\varepsilon_{QW}(\omega) = \varepsilon \left(1 - \frac{\omega_{P\alpha}^2}{\omega^2 - \omega_\alpha^2} \right). \quad (110)$$

The result (109) is very similar to the effective dielectric constant obtained by Zeluzny and Nalewajko.¹⁴ This result arises naturally from the initial assumption that the heterostructure is much smaller than the wavelength of light. However, in our case, the geometrical overlap factor $f_\alpha^o f_\alpha^w$ contains a quantum correction due to the shape of the wave functions.

The model developed so far is purely Hamiltonian, and the dissipation has not been included. The dissipation can be introduced through a coupling with a reservoir of harmonic oscillators. Such a model has been considered, for instance, in Refs. 17 and 18. In particular, the method of Ref. 18 leads to a dielectric function of the form

$$\varepsilon_{QW}(\omega) = \varepsilon \left(1 - \frac{\omega_{P\alpha}^2}{\omega^2 + i\Gamma_\alpha \omega - \omega_\alpha^2} \right). \quad (111)$$

Here, Γ_α is the linewidth of the intersubband plasmon modes, which can be determined in a phenomenological way, i.e., from absorption measurements.¹⁹

On the basis of the results from the previous section, we can obtain an approximation for the dielectric constant by replacing the effective plasma thickness L_{eff}^α with its maximum value L_{QW}/f_α^o [see Eq. (103)]. We can call this substitution the ‘‘semiclassical approximation’’ since it leads to a plasma self-energy provided by the classical expression, as seen from Eq. (106). This leads to the widespread expression for the heterostructure dielectric constant²²

$$\varepsilon_{QW,\text{cl}}(\omega) = \varepsilon \left(1 - \frac{\tilde{\omega}_{P\alpha}^2}{\omega^2 + i\Gamma_\alpha \omega - \omega_\alpha^2} \right), \quad (112)$$

$$\tilde{\omega}_{P\alpha}^2 = \frac{f_\alpha^o e^2 \Delta N_\alpha}{\varepsilon \varepsilon_0 m^* S L_{QW}}. \quad (113)$$

In this limit, we obtain exactly the effective medium constant from Ref. 14 since, in this case, the product $f_\alpha^o f_\alpha^w$ is replaced with L_{QW}/L_{cav} , which is independent from the particular intersubband transition. From Sec. IV B, it is clear that the semiclassical approximation assumes that the intersubband polarization is constant inside the heterostructure slab, and zero everywhere else.

Including more than one transition in the definition of the dielectric constant is not not trivial since one is obliged to diagonalize the full plasma Hamiltonian (53), taking into account the coupling between the different intersubband plasmons. The semiclassical approximation allows us to write a simple analytical expression for the multitransition dielectric function

$$\varepsilon_{QW,\text{cl}}(\omega) = \varepsilon \left(1 - \sum_\alpha \frac{\tilde{\omega}_{P\alpha}^2}{\omega^2 + i\Gamma_\alpha \omega_{\mathbf{q}} - \omega_\alpha^2} \right). \quad (114)$$

This result is demonstrated in Appendix E.

V. CONCLUSION

In summary, we have provided a theoretical description of the light-matter interaction for the intersubband transitions in

the electrical dipole gauge. We showed that, by introducing a microscopic expression for the intersubband polarization field $\hat{\mathbf{P}}(\mathbf{r})$, the Power-Zienau-Woolley Hamiltonian provides a suitable framework for the study of the interaction between the collective electronic excitations and light. This description is very general and applies to an arbitrary electronic potential once the corresponding single-particle wave functions are known. In particular, it can be used in the case of the ultrastrong-coupling regime in the limit of very high electronic densities and high overlap factors between the quantum well medium and the microcavity mode.

The physical interpretation of the dipolar interaction Hamiltonian is straightforward. The linear part of the Hamiltonian \hat{H}_{11} describes the coupling of the electronic excitations with the cavity electromagnetic field. The quadratic part \hat{H}_{12} contains the depolarization effect (the effect of an oscillating current on itself) and the coupling between plasmons from different transitions. The plasma energy described by the term \hat{H}_{12} leads to the no-go theorem for intersubband transitions. This energy has a close analogy to the electromagnetic dipole self-energy of a two-level system,¹⁰ which plays an important role for the estimation of the radiative corrections of atomic transitions.^{1,40}

When the dipolar Hamiltonian is transformed back in the Coulomb gauge, it provides the Coulomb interaction terms of the system including image charge effects arising from the boundary conditions on the cavity walls. This has been discussed for a truncated Hamiltonian describing a single intersubband transition interacting with a TM₀ mode of a double-metal waveguide. In this case, we find that the weights of the scalar potential V and the \mathbf{A}^2 term of the Coulomb gauge version of the Hamiltonian are governed by the geometrical overlap factor f_{α}^w . Our study completes the theoretical framework of the ultrastrong coupling, introduced in Ref. 4, where only on the vector potential part \mathbf{A}^2 was considered. We found that this study is justified for cavities with filling factors close to unity. A more general PZW back transformation, which uses the whole basis of guided modes and the full set of intersubband transitions, will be discussed elsewhere.

We believe that the approach developed here, based on operator formalism to describe the collective intersubband excitations, provides a compact and useful description, which could allow further studies of quantum electrodynamical effects inserted in solid-state systems.

ACKNOWLEDGMENTS

The authors acknowledge very useful discussions with C. Ciuti, D. Hagenmuller, and S. De Liberato. We also acknowledge financial support from the ERC grant ‘‘ADEQUATE.’’

APPENDIX A: VACUUM FIELD AMPLITUDE OF THE GUIDED MODES

In this Appendix, we derive the vacuum normalization constant $A_{\mathbf{q}}$ [Eq. (7)] by taking into account the multilayered geometry of the guided mode stack. We also comment on the special treatment of metallic boundaries of the guiding structure.

We start by expressing the volume integral (2) as a function of the TM-polarized field components (4)–(6):

$$\begin{aligned} \frac{\mu_0}{2} \int \hat{\mathbf{H}}^2 d^3\mathbf{r} &= \frac{\mu_0}{2} \int \hat{\mathbf{H}}\hat{\mathbf{H}}^\dagger d^3\mathbf{r} \\ &= S \sum_{\mathbf{q}} A_{\mathbf{q}}^2 (a_{\mathbf{q}}^\dagger a_{\mathbf{q}} + a_{\mathbf{q}} a_{\mathbf{q}}^\dagger + a_{\mathbf{q}} a_{-\mathbf{q}} + a_{\mathbf{q}}^\dagger a_{-\mathbf{q}}^\dagger) \\ &\quad \times \frac{\mu_0}{2} \int f_{\mathbf{q}}^2(z) dz, \end{aligned} \quad (\text{A1})$$

$$\begin{aligned} \int \frac{1}{2\varepsilon_0\varepsilon(z)} \hat{\mathbf{D}}_z^2 d^3\mathbf{r} &= \int \frac{1}{2\varepsilon_0\varepsilon(z)} \hat{\mathbf{D}}_z \hat{\mathbf{D}}_z^\dagger d^3\mathbf{r} \\ &= S \sum_{\mathbf{q}} A_{\mathbf{q}}^2 (a_{\mathbf{q}}^\dagger a_{\mathbf{q}} + a_{\mathbf{q}} a_{\mathbf{q}}^\dagger - a_{\mathbf{q}} a_{-\mathbf{q}} - a_{\mathbf{q}}^\dagger a_{-\mathbf{q}}^\dagger) \\ &\quad \times \frac{\mathbf{q}^2}{\omega_{\text{cq}}^2} \int \frac{1}{2\varepsilon_0\varepsilon(z)} f_{\mathbf{q}}^2(z) dz, \end{aligned} \quad (\text{A2})$$

$$\begin{aligned} \int \frac{1}{2\varepsilon_0\varepsilon(z)} \hat{\mathbf{D}}_{\parallel}^2 d^3\mathbf{r} &= \int \frac{1}{2\varepsilon_0\varepsilon(z)} \hat{\mathbf{D}}_{\parallel} \hat{\mathbf{D}}_{\parallel}^\dagger d^3\mathbf{r} \\ &= S \sum_{\mathbf{q}} A_{\mathbf{q}}^2 (a_{\mathbf{q}}^\dagger a_{\mathbf{q}} + a_{\mathbf{q}} a_{\mathbf{q}}^\dagger - a_{\mathbf{q}} a_{-\mathbf{q}} - a_{\mathbf{q}}^\dagger a_{-\mathbf{q}}^\dagger) \\ &\quad \times \frac{1}{\omega_{\text{cq}}^2} \int \frac{1}{2\varepsilon_0\varepsilon(z)} \left(\frac{df_{\mathbf{q}}}{dz} \right)^2 dz. \end{aligned} \quad (\text{A3})$$

To derive these expressions, we have used the parity of ω_{cq} and $A_{\mathbf{q}}$ as respect to \mathbf{q} and $\mathbf{e}_{-\mathbf{q}} = -\mathbf{e}_{\mathbf{q}}$. We have also used the orthogonality of the two-dimensional space harmonics $\exp(i\mathbf{q}\mathbf{r}_{\parallel})/\sqrt{S}$.

To obtain the proper normalization of the electromagnetic field, we first show the following identity:

$$I = \int dz \left\{ \frac{\mu_0}{2} f_{\mathbf{q}}^2 - \frac{1}{2\varepsilon_0\varepsilon(z)} \left[\frac{\mathbf{q}^2}{\omega_{\text{cq}}^2} f_{\mathbf{q}}^2 + \left(\frac{df_{\mathbf{q}}}{dz} \right)^2 \right] \right\} = 0. \quad (\text{A4})$$

For the demonstration, we use the Helmholtz equation (9). Let us consider the i th layer, then by definition $\varepsilon(z) = \varepsilon_i$ is constant. By multiplying Eq. (9) by $f_{\mathbf{q}}$ and integrating across the i th layer, we obtain

$$I_i = -\frac{1}{\varepsilon_0\varepsilon_i} f_{\mathbf{q}} \frac{df_{\mathbf{q}}}{dz} \Big|_{i+} + \frac{1}{\varepsilon_0\varepsilon_i} f_{\mathbf{q}} \frac{df_{\mathbf{q}}}{dz} \Big|_{i-}, \quad (\text{A5})$$

$$I_i = \int_i dz \left\{ \mu_0 f_{\mathbf{q}}^2 - \frac{1}{\varepsilon_0\varepsilon_i} \left[\frac{\mathbf{q}^2}{\omega_{\text{cq}}^2} f_{\mathbf{q}}^2 + \left(\frac{df_{\mathbf{q}}}{dz} \right)^2 \right] \right\}. \quad (\text{A6})$$

Here, we have also used that $\varepsilon_0\mu_0 = 1/c^2$, and the symbol $i\pm$ means the upper (lower) side of the layer. By using the boundary conditions of the electromagnetic field

$$f_{\mathbf{q}}|_{i-} = f_{\mathbf{q}}|_{(i+)+}, \quad (\text{A7})$$

$$\frac{1}{\varepsilon_i} \frac{df_{\mathbf{q}}}{dz} \Big|_{i-} = \frac{1}{\varepsilon_{i+1}} \frac{df_{\mathbf{q}}}{dz} \Big|_{(i+)+}, \quad (\text{A8})$$

and the fact that $I = 1/2 \sum_i I_i$, we finally obtain

$$I = -\frac{1}{2\varepsilon_0\varepsilon_U} f_{\mathbf{q}} \frac{df_{\mathbf{q}}}{dz} \Big|_U + \frac{1}{2\varepsilon_0\varepsilon_D} f_{\mathbf{q}} \frac{df_{\mathbf{q}}}{dz} \Big|_D, \quad (\text{A9})$$

where $U(D)$ denotes the upper (lower) boundary of the multilayer. Either one or the two boundaries go to infinity; then the field and its derivative go to zero. The other option is to take metallic boundaries. Since in the mid- and far- infrared ranges the dielectric constant of the metals ε_M is very high, we can adopt perfect metal boundary conditions, where $|\varepsilon_M| \rightarrow \infty$. We can then neglect the contribution of the field from the metallic layers in the integral (2). In all cases, the identity (A4) is proven. Thanks to this identity, the antiresonant terms in the photon Hamiltonian cancel, and the remaining term is simplified to

$$\sum_{\mathbf{q}} 2\mu_0 S L_{\mathbf{q}} A_{\mathbf{q}}^2 (a_{\mathbf{q}}^\dagger a_{\mathbf{q}} + 1/2). \quad (\text{A10})$$

Following standard textbooks,¹⁰ the prefactor should correspond to the energy quantum of the guided mode $\hbar\omega_{c\mathbf{q}}$, which leads to Eq. (7).

Although we used perfect metal boundary conditions for the normalization of the vacuum field amplitude $A_{\mathbf{q}}$, we can still describe the effects of the finite metal permittivity ε_M in our model. As an example, consider the current experimental situation where the multilayer is constituted by a surface plasmon waveguide, obtained by depositing a metal layer on a semiconductor substrate. We suppose the metal-semiconductor interface to be at $z = 0$. In the semiconductor, the mode profile is described by an exponential function $f_{\mathbf{q}}(z) = e^{\gamma_{\mathbf{q}} z}$ for $z < 0$, with $\gamma_{\mathbf{q}}$ the decay length of the surface plasmon mode into the semiconductor. Let ε be the dielectric constant of the semiconductor, then we have⁴¹

$$\frac{\omega_{c\mathbf{q}}^2}{c^2} = \mathbf{q}^2 \left| \frac{1}{\varepsilon} + \frac{1}{\varepsilon_M} \right|, \quad (\text{A11})$$

$$\gamma_{\mathbf{q}} = \varepsilon \frac{\omega_{c\mathbf{q}}}{c} \left| \frac{1}{\varepsilon} + \frac{1}{\varepsilon_M} \right|. \quad (\text{A12})$$

Using the above prescription, we consider the field in the metal to vanish, but we keep the expression of the finite dielectric function ε_M in the dispersion relations above. We then have $L_{\mathbf{q}} = 1/2\gamma_{\mathbf{q}}$, and the quantum amplitude of the surface plasmon mode becomes

$$A_{\mathbf{q}} = \left(\frac{\varepsilon_0 \varepsilon c \hbar \omega_{c\mathbf{q}}^2}{S |\varepsilon + \varepsilon_M|^{1/2}} \right)^{1/2} \quad (\text{A13})$$

We see that in the far-infrared domain, where $\omega_{c\mathbf{q}} \rightarrow 0$ and ε_M is very large and negative, both spontaneous emission and the strong-coupling phenomena are unfavored since $A_{\mathbf{q}}$ has vanishingly small values. On the contrary, the photon electric amplitude $A_{\mathbf{q}}$ can be enhanced in a microcavity resonator.

APPENDIX B: DERIVATION OF THE POLARITON DOT HAMILTONIAN

We first write the linear part of the interaction Hamiltonian (3) by using the expressions (27), (61), and the definition (64):

$$H_{11} = i \sum_{\alpha, m} \sqrt{\frac{\hbar \omega_{cm}}{2\varepsilon \varepsilon_0 S L_{cav}}} z_{\alpha} (a_m^\dagger - a_m) \times \sum_{\mathbf{q}} [B_{\alpha\mathbf{q}}^\dagger \langle \mathbf{q} | u_m \rangle + B_{\alpha\mathbf{q}} \langle -\mathbf{q} | u_m \rangle]. \quad (\text{B1})$$

Since the function $u_m(\mathbf{r}_{\parallel})$ is real, we have $\langle -\mathbf{q} | u_m \rangle = \langle u_m | \mathbf{q} \rangle$, and therefore we can use the transformation law (65) and its Hermitian conjugate to obtain

$$H_{11} = i \sum_{\alpha, m} \sqrt{\frac{\hbar \omega_{cm}}{2\varepsilon \varepsilon_0 S L_{cav}}} z_{\alpha} (a_m^\dagger - a_m) (B_{\alpha m}^\dagger + B_{\alpha m}). \quad (\text{B2})$$

In order to transform the quadratic part (31), we use the inverse transformations

$$B_{\alpha\mathbf{q}}^\dagger = \sum_m \langle u_m | \mathbf{q} \rangle B_{\alpha m}^\dagger, \quad (\text{B3})$$

$$B_{\alpha\mathbf{q}} = \sum_m \langle \mathbf{q} | u_m \rangle B_{\alpha m}, \quad (\text{B4})$$

and therefore

$$\begin{aligned} & \sum_{\mathbf{q}} (B_{\alpha\mathbf{q}}^\dagger + B_{\alpha-\mathbf{q}}) (B_{\beta-\mathbf{q}}^\dagger + B_{\beta\mathbf{q}}) \\ &= \sum_{\mathbf{q}, m, m'} (\langle u_m | \mathbf{q} \rangle B_{\alpha m}^\dagger + \langle -\mathbf{q} | u_m \rangle B_{\alpha m}) \\ & \quad \times (\langle u_{m'} | -\mathbf{q} \rangle B_{\beta m'}^\dagger + \langle \mathbf{q} | u_{m'} \rangle B_{\beta m'}). \end{aligned} \quad (\text{B5})$$

Using once again the relation $\langle -\mathbf{q} | u_m \rangle = \langle u_m | \mathbf{q} \rangle$ and the closure relation $\sum_{\mathbf{q}} |\mathbf{q}\rangle \langle \mathbf{q}| = 1$ along with the orthogonality condition $\langle u_m | u_{m'} \rangle = \delta_{mm'}$, it is straightforward to transform the expression (B5) into

$$\sum_m (B_{\alpha m}^\dagger + B_{\alpha m}) (B_{\beta m}^\dagger + B_{\beta m}). \quad (\text{B6})$$

We then use exactly the same bosonization approach as in Sec. III A to arrive at the Hamiltonian (67).

APPENDIX C: LONG-WAVELENGTH LIMIT OF THE COULOMB INTERACTION

In order to show that the last term of Eq. (78) has the form of the Coulomb interaction, we first reexpress it through the B operators defined in Sec. II D:

$$\begin{aligned} & \sum_{\mathbf{q}} \frac{\hbar \omega_p^2}{4\omega_{21}} (b_{\mathbf{q}}^\dagger + b_{-\mathbf{q}}) (b_{-\mathbf{q}}^\dagger + b_{\mathbf{q}}) \\ &= \frac{1}{2S\varepsilon\varepsilon_0} \frac{e^2 \hbar^2}{4m^{*2} \omega_{21}^2} I_{12,12} \\ & \quad \times \sum_{\mathbf{q}} (B_{21\mathbf{q}}^\dagger + B_{21-\mathbf{q}}) (B_{21-\mathbf{q}}^\dagger + B_{21\mathbf{q}}). \end{aligned} \quad (\text{C1})$$

We first use the Vinter's identity^{7,42}

$$\begin{aligned} & \frac{\hbar^2}{4m^{*2} \omega_{21}^2} I_{12,12} \\ &= - \int \int_{-\infty}^{+\infty} dz dz' \phi_1(z) \phi_2(z) |z - z'| \phi_1(z') \phi_2(z') \end{aligned} \quad (\text{C2})$$

and we recognize the prefactor of (C1) to be exactly the long-wavelength limit of the Coulomb interaction matrix element

$V_{\mathbf{q} \rightarrow \mathbf{0}}^{\lambda\mu, \mu'\lambda'}$:

$$V_{\mathbf{q} \rightarrow \mathbf{0}}^{\lambda\mu, \mu'\lambda'} = -\frac{e^2}{2S\epsilon\epsilon_0} \int \int_{-\infty}^{+\infty} dz dz' \phi_\lambda(z) \times \phi_\mu(z) |z - z'| \phi_{\mu'}(z') \phi_{\lambda'}(z'). \quad (\text{C3})$$

Note that we have $V_{\mathbf{q} \rightarrow \mathbf{0}}^{12,12} = V_{\mathbf{q} \rightarrow \mathbf{0}}^{21,21} = V_{\mathbf{q} \rightarrow \mathbf{0}}^{21,12} = V_{\mathbf{q} \rightarrow \mathbf{0}}^{12,21}$, so we recover only the matrix elements that describe the interaction of electrons between subbands 1 and 2, as should be expected.

Next, by using the fermionic commutation rules, we can easily rearrange the binary products of B operators into four c -operator products:

$$\sum_{\mathbf{q}} B_{21\mathbf{q}}^\dagger B_{21-\mathbf{q}}^\dagger = \sum_{\mathbf{q}, \mathbf{k}, \mathbf{k}'} c_{2\mathbf{k}+\mathbf{q}}^\dagger c_{2\mathbf{k}'-\mathbf{q}}^\dagger c_{1\mathbf{k}'} c_{1\mathbf{k}}, \quad (\text{C4})$$

$$\sum_{\mathbf{q}} B_{21\mathbf{q}} B_{21-\mathbf{q}} = \sum_{\mathbf{q}, \mathbf{k}, \mathbf{k}'} c_{1\mathbf{k}+\mathbf{q}}^\dagger c_{1\mathbf{k}'-\mathbf{q}}^\dagger c_{2\mathbf{k}'} c_{2\mathbf{k}}, \quad (\text{C5})$$

$$\sum_{\mathbf{q}} B_{21\mathbf{q}}^\dagger B_{21\mathbf{q}} = \sum_{\mathbf{q}, \mathbf{k}, \mathbf{k}'} c_{2\mathbf{k}+\mathbf{q}}^\dagger c_{1\mathbf{k}'-\mathbf{q}}^\dagger c_{2\mathbf{k}'} c_{1\mathbf{k}} + \sum_{\mathbf{q}, \mathbf{k}} c_{2\mathbf{k}+\mathbf{q}}^\dagger c_{2\mathbf{k}+\mathbf{q}}, \quad (\text{C6})$$

$$\sum_{\mathbf{q}} B_{21\mathbf{q}} B_{21\mathbf{q}}^\dagger = \sum_{\mathbf{q}, \mathbf{k}, \mathbf{k}'} c_{1\mathbf{k}+\mathbf{q}}^\dagger c_{2\mathbf{k}'-\mathbf{q}}^\dagger c_{1\mathbf{k}'} c_{2\mathbf{k}} + \sum_{\mathbf{q}, \mathbf{k}} c_{1\mathbf{k}+\mathbf{q}}^\dagger c_{1\mathbf{k}+\mathbf{q}}. \quad (\text{C7})$$

Note that the sum of the pair terms in Eqs. (C6) and (C7) simply acts as the identity operator in the two-subband subspace and therefore can be ignored. The remaining four operator terms can be regrouped in order to provide the long-wavelength expansion of the Coulomb potential \bar{V} for our problem:

$$\bar{V} = (1 - f_{21}^o f_{21}^w) \sum_{\substack{\mathbf{q}, \mathbf{k}, \mathbf{k}' \\ [\lambda\mu, \mu'\lambda']}} V_{\mathbf{q} \rightarrow \mathbf{0}}^{\lambda\mu, \mu'\lambda'} c_{\lambda\mathbf{k}+\mathbf{q}}^\dagger c_{\mu\mathbf{k}'-\mathbf{q}}^\dagger c_{\mu'\mathbf{k}'} c_{\lambda'\mathbf{k}}. \quad (\text{C8})$$

The symbol $[\lambda\mu, \mu'\lambda']$ means that the sum runs only along the four Coulomb matrix elements mentioned above. The final result (C8) can be interpreted as a dipole-dipole interaction, where the oscillating intersubband dipole moments interact with each other through their local field.³³

APPENDIX D: PROPERTIES OF THE POLARITON DISPERSION

The eigenvalue equation for the polariton problem is [Eq. (87)]

$$(\omega^2 - \tilde{\omega}_\alpha^2)(\omega^2 - \omega_c^2) = f_\alpha^o f_\alpha^w \omega_p^2 \omega_c^2. \quad (\text{D1})$$

For simplicity, we have dropped the wave vector index \mathbf{q} . The real roots of Eq.(D1) are obtained from

$$\omega_\pm^2 = \frac{1}{2}(\omega_c^2 + \tilde{\omega}_\alpha^2 \pm \sqrt{\Delta}), \quad (\text{D2})$$

$$\Delta = (\omega_c^2 + \tilde{\omega}_\alpha^2)^2 - 4\omega_c^2 \tilde{\omega}_\alpha^2. \quad (\text{D3})$$

From these equations, it is easy to deduce

$$\frac{d\omega_\pm}{d\omega_c^2} = \frac{1}{4\omega_\pm} \left(1 \pm \frac{d\sqrt{\Delta}}{d\omega_c^2} \right). \quad (\text{D4})$$

The minimal splitting is obtained from

$$\frac{d(\omega_+ - \omega_-)}{d\omega_c^2} = 0. \quad (\text{D5})$$

Multiplying this equation by $\omega_+ - \omega_-$ and using (D4), we obtain

$$(\omega_+ - \omega_-)^2 = \frac{\omega_+^2 - \omega_-^2}{2\sqrt{\Delta}} \frac{d\sqrt{\Delta}}{d\omega_c^2}. \quad (\text{D6})$$

To transform this equation, we use the following relations:

$$\omega_+^2 - \omega_-^2 = \sqrt{\Delta}, \quad (\text{D7})$$

$$\omega_+^2 + \omega_-^2 = \omega_c^2 + \tilde{\omega}_\alpha^2, \quad (\text{D8})$$

$$\omega_+^2 \omega_-^2 = \omega_c^2 \tilde{\omega}_\alpha^2. \quad (\text{D9})$$

The first is an immediate corollary from (D2), while the second and the third are the Newton formulas for Eq. (D1). We then have

$$\begin{aligned} 2(\omega_+ - \omega_-)^2 &= 2(\omega_+^2 + \omega_-^2 - 2\omega_+ \omega_-) \\ &= 2(\omega_c^2 + \tilde{\omega}_\alpha^2 - 2\omega_c \tilde{\omega}_\alpha) = \frac{d\sqrt{\Delta}}{d\omega_c^2} \\ &= 2(\omega_c^2 + \tilde{\omega}_\alpha^2) - 4\tilde{\omega}_\alpha^2. \end{aligned} \quad (\text{D10})$$

To obtain the last line, we have derived Eq. (D3) with respect to ω_c^2 . This equation clearly leads to the result

$$\frac{d(\omega_+ - \omega_-)}{d\omega_c^2} = 0 \Leftrightarrow \omega_c = \tilde{\omega}_\alpha. \quad (\text{D11})$$

Furthermore, we can express the minimal splitting

$$\min(\omega_+ - \omega_-)^2 = \tilde{\omega}_\alpha^2 - \tilde{\omega}_\alpha^2 = f_\alpha^o f_\alpha^w \omega_p^2. \quad (\text{D12})$$

This is the result stated in Eqs. (92) and (93).

APPENDIX E: SEMICLASSICAL PLASMA HAMILTONIAN

In this Appendix, we consider the plasma Hamiltonian in the semiclassical approximation discussed in the end of Sec. IV C. It will be shown that this Hamiltonian leads to the semiclassical dielectric constant (114).

In the semiclassical approximation, it is assumed that the intersubband polarization is constant along the heterostructure slab. We can then approximate the current-current correlation function by the first order in the expansion (100) described in Sec. IV B:

$$\begin{aligned} \int_{-\infty}^{+\infty} \xi_\alpha(z) \xi_\beta(z) dz &\approx \frac{1}{L_{\text{QW}}} \int_0^{L_{\text{QW}}} \xi_\alpha(z) dz \int_0^{L_{\text{QW}}} \xi_\beta(z) dz \\ &= \frac{2m^*}{\hbar} \sqrt{\omega_\alpha \omega_\beta f_\beta^o f_\alpha^o}. \end{aligned} \quad (\text{E1})$$

This is equivalent to use a suitably averaged microscopic response in the quantum well slab. With the use of (E1), we obtain the following expressions for the coefficients that enter the plasma Hamiltonian:

$$L_{\text{eff}}^\alpha = L_{\text{QW}} / f_\alpha^o, \quad (\text{E2})$$

$$\tilde{\omega}_{P_\alpha}^2 = \frac{e^2 f_\alpha^o \Delta N_\alpha}{\epsilon \epsilon_0 m^* S L_{\text{QW}}}, \quad (\text{E3})$$

$$C_{\alpha, \beta} = 1. \quad (\text{E4})$$

We consider first the matter part of the plasma Hamiltonian, which is rewritten as

$$H = \sum_{\alpha, \mathbf{q}} \hbar \tilde{\omega}_{\alpha} p_{\alpha \mathbf{q}}^{\dagger} p_{\alpha \mathbf{q}} + \sum_{\alpha \neq \beta, \mathbf{q}} \frac{\hbar \bar{\omega}_{P\alpha} \bar{\omega}_{P\beta}}{2\sqrt{\tilde{\omega}_{\alpha} \tilde{\omega}_{\beta}}} (p_{\alpha \mathbf{q}}^{\dagger} + p_{\alpha - \mathbf{q}})(p_{\beta - \mathbf{q}}^{\dagger} + p_{\beta \mathbf{q}}). \quad (\text{E5})$$

Since the plasmon coupling coefficients are independent from the index \mathbf{q} , the latter is dropped in the equations, and (E5) is expressed in a more handy form:

$$H = \sum_{\alpha} \hbar \tilde{\omega}_{\alpha} p_{\alpha}^{\dagger} p_{\alpha} + \sum_{\alpha \neq \beta} \hbar \Omega_{\alpha\beta} (p_{\alpha}^{\dagger} + p_{\alpha})(p_{\beta}^{\dagger} + p_{\beta}), \quad (\text{E6})$$

$$\Omega_{\alpha\beta} = \Omega_{\beta\alpha} = \frac{\hbar \bar{\omega}_{P\alpha} \bar{\omega}_{P\beta}}{2\sqrt{\tilde{\omega}_{\alpha} \tilde{\omega}_{\beta}}}. \quad (\text{E7})$$

Let us consider N coupled plasmons; then, the Hopfield determinant of the resulting Hamiltonian is

$$\begin{vmatrix} \omega - \tilde{\omega}_1 & 0 & -\Omega_{12} & -\Omega_{12} & \dots & -\Omega_{1N} & -\Omega_{1N} \\ 0 & \omega + \tilde{\omega}_1 & \Omega_{12} & \Omega_{12} & \dots & \Omega_{1N} & \Omega_{1N} \\ -\Omega_{12} & -\Omega_{12} & \omega - \tilde{\omega}_2 & 0 & \dots & -\Omega_{2N} & -\Omega_{2N} \\ \Omega_{12} & \Omega_{12} & 0 & \omega + \tilde{\omega}_2 & \dots & \Omega_{2N} & \Omega_{2N} \\ \vdots & \vdots & \vdots & \vdots & \ddots & \vdots & \vdots \\ -\Omega_{1N} & -\Omega_{1N} & -\Omega_{2N} & -\Omega_{2N} & \dots & \omega - \tilde{\omega}_N & 0 \\ \Omega_{1N} & \Omega_{1N} & \Omega_{2N} & \Omega_{2N} & \dots & 0 & \omega + \tilde{\omega}_N \end{vmatrix}. \quad (\text{E8})$$

To simplify this determinant, we first add every impair row to the row above, then we subtract every impair column from the column on the left. This leads to the following simplified determinant:

$$\begin{vmatrix} \omega - \tilde{\omega}_1 & 2\tilde{\omega}_1 & 0 & 0 & \dots & 0 & 0 \\ 0 & \omega + \tilde{\omega}_1 & \Omega_{12} & 0 & \dots & \Omega_{1N} & 0 \\ 0 & 0 & \omega - \tilde{\omega}_2 & 2\tilde{\omega}_2 & \dots & 0 & 0 \\ \Omega_{12} & 0 & 0 & \omega + \tilde{\omega}_2 & \dots & \Omega_{2N} & 0 \\ \vdots & \vdots & \vdots & \vdots & \ddots & \vdots & \vdots \\ 0 & 0 & 0 & 0 & \dots & \omega - \tilde{\omega}_N & 2\tilde{\omega}_N \\ \Omega_{1N} & 0 & \Omega_{2N} & 0 & \dots & 0 & \omega + \tilde{\omega}_N \end{vmatrix}. \quad (\text{E9})$$

Let $\Delta_{[1, \dots, N]}$ be the determinant of N th order. By developing this determinant along the columns, we obtain the following recursive expression:

$$\begin{aligned} \Delta_{[1, \dots, N]} &= (\omega^2 - \tilde{\omega}_1^2) \Delta_{[2, \dots, N]} - 2^2 \sum_i^N \tilde{\omega}_1 \tilde{\omega}_i \Omega_{1i} \Omega_{i1} \Delta_{[2, \dots, N]/[i]} \dots \\ &\quad - n! 2^{n+1} \sum_{\overline{i_1, i_2, \dots, i_n}} \tilde{\omega}_1 \tilde{\omega}_{i_1}, \dots, \tilde{\omega}_{i_n} \Omega_{1i_1} \Omega_{i_1 i_2}, \dots, \Omega_{i_n 1} \Delta_{[2, \dots, N]/[i_1, i_2, \dots, i_n]} \dots \\ &\quad - (N-1)! 2^N \tilde{\omega}_1 \tilde{\omega}_2, \dots, \tilde{\omega}_N \Omega_{12} \Omega_{23}, \dots, \Omega_{N1} \end{aligned} \quad (\text{E10})$$

with $\Delta_{[2, \dots, N]/[i_1, i_2, \dots, i_n]}$ being the determinant of order $N-1-n$, excluding the transitions i_1, i_2, \dots, i_n . The notation $\overline{i_1, i_2, \dots, i_n}$ means that the sum does not contain repetitive indexes. Using the definition (E7), the determinant is easily rewritten as

$$\begin{aligned} \Delta_{[1, \dots, N]} &= (\omega^2 - \tilde{\omega}_1^2) \Delta_{[2, \dots, N]} - \sum_i^N \tilde{\omega}_{P1}^2 \tilde{\omega}_{Pi}^2 \Delta_{[2, \dots, N]/[i]} \dots - n! \sum_{\overline{i_1, i_2, \dots, i_n}} \tilde{\omega}_{P1}^2 \tilde{\omega}_{Pi_1}^2, \dots, \tilde{\omega}_{Pi_n}^2 \Delta_{[2, \dots, N]/[i_1, i_2, \dots, i_n]} \dots \\ &\quad - (N-1)! \tilde{\omega}_{P1}^2 \tilde{\omega}_{P2}^2, \dots, \tilde{\omega}_{PN}^2. \end{aligned} \quad (\text{E11})$$

Having expressed the N th-order determinant as a function of lower-order ones, we make the following recursive assumption for $n < N$:

$$\Delta_{[1,\dots,n]} = \prod_{i=1}^n (\omega^2 - \omega_i^2) \left(1 - \sum_{i=1}^n \frac{\bar{\omega}_{Pi}^2}{\omega^2 - \omega_i^2} \right). \quad (\text{E12})$$

Let us denote $x_i = \bar{\omega}_{Pi}^2/(\omega^2 - \omega_i^2)$, then our recursive hypothesis implies

$$\begin{aligned} \Delta_{[1,\dots,N]} = & \prod_{i=1}^N (\omega^2 - \omega_i^2) \left[(1 - x_1) \left(1 - \sum_{i=2}^N x_i \right) - \sum_{i=2}^N x_1 x_i \left(1 - \sum_{k=2, k \neq i}^N x_k \right) \dots - n! \right. \\ & \left. \times \sum_{i_1, i_2, \dots, i_n} x_1 x_{i_1} \dots x_{i_n} \left(1 - \sum_{k=2, k \neq i_1, i_2, \dots, i_n}^N x_k \right) \dots - (N-1)! x_1 x_2 \dots x_N \right]. \end{aligned} \quad (\text{E13})$$

We can easily show that all the terms in this sum that imply high orders of the x_i cancel two by two, except the linear terms, which completes our recursive demonstration. The final result can be cast in the form

$$\Delta_{[1,\dots,N]} = \frac{\varepsilon_{\text{QW,cl}}(\omega)}{\varepsilon} \prod_{i=1}^N (\omega^2 - \omega_i^2), \quad (\text{E14})$$

where $\varepsilon_{\text{QW,cl}}(\omega)$ is the semiclassical multiband dielectric constant, provided by Eq. (114). Therefore, the coupled plasmonic eigenmodes of the Hamiltonian (E5) are provided by the zeros of the dielectric function $\varepsilon_{\text{QW,cl}}(\omega)$.

If we now add the light-matter interaction with a single photonic mode, similar reasoning leads to the Hopfield determinant

$$\Delta(\omega) = \frac{\varepsilon_{\text{QW,cl}}(\omega)}{\varepsilon} \left(\omega^2 - \omega_c^2 \frac{\varepsilon}{\varepsilon_{\text{eff,cl}}(\omega)} \right) \prod_{i=1}^N (\omega^2 - \omega_i^2) \quad (\text{E15})$$

with $\varepsilon_{\text{eff,cl}}(\omega)$ the classical effective medium constant defined by

$$\frac{1}{\varepsilon_{\text{eff,cl}}(\omega)} = \frac{f_w}{\varepsilon_{\text{QW,cl}}(\omega)} + \frac{1 - f_w}{\varepsilon}. \quad (\text{E16})$$

Here, $f_w = L_{\text{QW}}/L_{\text{cav}}$ is the filling factor of the quantum well (heterostructure) in the cavity, which is independent from the intersubband transition in this approximation.

From a mathematical point of view, the analytical diagonalization of the problem was obtained thanks to the relation $C_{\alpha,\beta} = 1$. This would not be possible in the general case, and yet it is clear that the Hopfield determinant of the Hamiltonian (53) is a polynomial of $2 \times (N + 1)$ th degree. Therefore, we can still use the definition (107) to compute numerically the exact quantum effective dielectric constant of the problem.

-
- ¹M. Babiker and R. Loudon, *Proc. R. Soc. London, Ser. A* **385**, 439 (1983).
²E. A. Power and S. Zienau, *Nuovo Cimento* **6**, 7 (1957).
³R. G. Woolley, *Proc. R. Soc. London, Ser. A* **321**, 557 (1971).
⁴C. Ciuti, G. Bastard, and I. Carusotto, *Phys. Rev. B* **72**, 115303 (2005).
⁵D. Dini, R. Kohler, A. Tredicucci, G. Biasiol, and L. Sorba, *Phys. Rev. Lett.* **90**, 116401 (2003).
⁶Y. Todorov, A. M. Andrews, R. Colombelli, S. De Liberato, C. Ciuti, P. Klang, G. Strasser, and C. Sirtori, *Phys. Rev. Lett.* **105**, 196402 (2010).
⁷T. Ando, A. B. Fowler, and F. Stern, *Rev. Mod. Phys.* **52**, 437 (1982).
⁸J. Keeling, *J. Phys.: Condens. Matter* **19**, 295213 (2007).
⁹D. E. Nikonov, A. Imamoglu, L. V. Butov, and H. Schmidt, *Phys. Rev. Lett.* **79**, 4633 (1997).
¹⁰C. Cohen-Tannoudji, J. Dupont-Roc, and G. Grynberg, *Photons et Atomes* (EDP Sciences, Paris, 2001).
¹¹P. Jouy, A. Vasanelli, Y. Todorov, A. Delteil, G. Biasiol, L. Sorba, and C. Sirtori, *Appl. Phys. Lett.* **98**, 231114 (2011).
¹²I. Bialynicki-Birula and K. Rzażnewski, *Phys. Rev. A* **19**, 301 (1979).
¹³P. Nataf and C. Ciuti, *Nat. Commun.* **1**, 72 (2010).
¹⁴M. Zaluzny and C. Nalewajko, *Phys. Rev. B* **59**, 13043 (1999).
¹⁵S. S. Scheel, L. Knöll, and D.-G. Welsch, *Coherence and Statistics of Photons and Atoms* (Wiley, New York, 2001).
¹⁶L. G. Suttorp, *J. Phys. A: Math. Theor.* **40**, 3697 (2007).
¹⁷B. Huttner and S. M. Barnett, *Phys. Rev. A* **46**, 4306 (1992).
¹⁸S. M. Dutra and K. Furuya, *Phys. Rev. A* **57**, 3050 (1998).
¹⁹M. Helm, in *Intersubband Transitions in Quantum Wells: Physics and Device Applications I*, edited by H. C. Liu and F. Capasso (Academic, San Diego, 2000).
²⁰G. D. Mahan, *Phys. Rev. B* **82**, 165318 (2010).
²¹David A. Dahl and L. J. Sham, *Phys. Rev. B* **16**, 651 (1977).
²²L. Wendler and E. Kändler, *Phys. Status Solidi B* **177**, 9 (1993).
²³L. Landau and E. Lifchitz, *Electrodynamics of Continuous Media* (Mir, Moscow, 1969).
²⁴R. Resta, *J. Phys.: Condens. Matter* **22**, 123201 (2010).
²⁵C. Sirtori, F. Capasso, J. Faist, and S. Scandolo, *Phys. Rev. B* **50**, 8663 (1994).

- ²⁶S. De Liberato and C. Ciuti, *Phys. Rev. Lett.* **102**, 136403 (2009).
- ²⁷S. De Liberato and C. Ciuti, *Phys. Rev. B* **79**, 075317 (2009).
- ²⁸F. Schwabl, *Advanced Quantum Mechanics* (Springer, Berlin, 2000).
- ²⁹Marie S-C. Luo, S. L. Chuang, S. Schmitt-Rink, and A. Pinczuk, *Phys. Rev. B* **48**, 11086 (1993).
- ³⁰M. Geiser, C. Walther, G. Scalari, M. Beck, M. Fischer, L. Nevou, and J. Faist, *Appl. Phys. Lett.* **97**, 191107 (2010).
- ³¹C. Cohen-Tannoudji, B. Diu, and F. Laloë, *Mécanique Quantique* (Hermann, Paris, 1977).
- ³²Y. Todorov, L. Toso, J. Teissier, A. M. Andrews, P. Klang, R. Colombelli, I. Sagnes, G. Strasser, and C. Sirtori, *Opt. Express* **18**, 13886 (2010).
- ³³J. J. Hopfield, *Phys. Rev.* **112**, 1555 (1958).
- ³⁴F. Bassani, J. J. Forney, and A. Quattropani, *Phys. Rev. Lett.* **39**, 1070 (1977).
- ³⁵A. A. Anappara, S. De Liberato, A. Tredicucci, C. Ciuti, G. Biasiol, L. Sorba, and F. Beltram, *Phys. Rev. B* **79**, 201303(R) (2009).
- ³⁶R. H. Dicke, *Phys. Rev.* **93**, 99 (1954).
- ³⁷M. Fox, *Quantum Optics* (Oxford University Press, New York, 2006).
- ³⁸L. C. Andreani, in *Proceedings of the International School of Physics Enrico Fermi, Course CL*, edited by B. Deveaud, A. Quattropani and P. Schwendimann (IOS Press, Amsterdam, 2003).
- ³⁹A. A. Anappara, A. Tredicucci, F. Beltram, G. Biasiol, and Lucia Sorba, *Appl. Phys. Lett.* **89**, 171109 (2006).
- ⁴⁰P. W. Milonni, *Phys. Rep.* **1**, 1 (1976).
- ⁴¹H. Raether, *Surface Plasmons* (Springer, Berlin, 1988).
- ⁴²B. Vinter, *Phys. Rev. B* **15**, 3947 (1977).